Small Molecules Restore Azole Activity Against Drug-Tolerant and Drug-Resistant *Candida* Isolates

Philip E. Alabi[1,2], Cécile Gautier[3], Thomas P. Murphy[4,5], Jason K. Sello[1,2*], Iuliana V. Ene[3,4*]

[1]Department of Chemistry, Brown University, Providence, RI

[2]Department of Pharmaceutical Chemistry, University of California San Francisco, San Francisco, CA

[3]Institut Pasteur, Université Paris Cité, Fungal Heterogeneity Lab, Paris, France

[4]Department of Molecular Microbiology and Immunology, Brown University, Providence, RI

[5]Current address: Cell Biology Program, Sloan Kettering Institute, New York, NY

*corresponding authors: iuliana.ene@pasteur.fr

jason.sello@ucsf.edu

key words: azole resistance, azole tolerance, 1,4-benzodiazepines, drug combinations

running title: 1,4-benzodiazepines potentiate azole antifungals

ABSTRACT

Each year, fungi cause more than 1.5 billion infections worldwide and have a devastating impact on human health, particularly in immunocompromised individuals or patients in intensive care units. The limited antifungal arsenal and emerging multidrug resistant species necessitate the development of new therapies. One strategy for combating drug resistant pathogens is the administration of molecules that restore fungal susceptibility to approved drugs. Accordingly, we carried out a screen to identify small molecules that could restore the susceptibility of pathogenic *Candida* species to azole antifungals. This screening effort led to the discovery of novel 1,4-benzodiazepines that restore fluconazole susceptibility in resistant isolates of *Candida albicans*, as evidenced by 100-1000-fold potentiation of fluconazole activity. This potentiation effect was also observed in azole-tolerant strains of *C. albicans* and in other pathogenic *Candida* species. The 1,4-benzodiazepines selectively potentiated different azoles, but not other antifungal drugs. A remarkable feature of the potentiation was that the combination of the 1,4-benzodiazepines with fluconazole was fungicidal, whereas fluconazole alone is fungistatic. Interestingly, the potentiators were not toxic to *C. albicans* in the absence of fluconazole, but inhibited virulence-associated filamentation of the fungus. We found that the combination of 1,4-benzodiazepines and fluconazole significantly enhanced host survival in a *Galleria mellonella* model of systemic fungal infection. Taken together, these observations validate a strategy wherein small molecules can restore the activity of highly used anti-infectives that have lost potency.

IMPORTANCE

In the last decade, we have been witnessing a higher incidence of fungal infections, an expansion of the fungal species capable of causing disease (e.g., *Candida auris*), as well

as increased antifungal drug resistance. Among human fungal pathogens, *Candida* species are a leading cause of invasive infections and are associated with high mortality rates. Azoles are the most widely used antifungals against *Candida* infections, yet the emergence and expansion of drug-resistant species have narrowed their clinical utility. In this work, we describe a set of novel 1,4-benzodiazepines that potentiate fluconazole and restore the susceptibility of azole-resistant and azole-tolerant *Candida* isolates. Interestingly, the potentiating 1,4-benzodiazepines were not toxic to fungal cells but inhibited their virulence associated filamentous growth. Furthermore, combinations of 1,4-benzodiazepines and fluconazole enhanced host survival in the *Galleria mellonella* model of systemic fungal infections. Accordingly, we propose the use of novel antifungal potentiators as a powerful strategy to restore fungal susceptibility to clinically approved drugs.

INTRODUCTION

Underlying more than 1.5 billion infections worldwide and an estimated 1.6 million deaths annually, fungal infections pose a significant threat to human health (1, 2). While most fungal infections are superficial, some can cause life-threatening invasive infections, especially in immunocompromised individuals (1, 3). Among pathogenic fungi, *Candida* species are especially concerning because they are the leading cause of systemic fungal infections with mortality rates reaching 50% (4, 5). The incidence of life-threatening *Candida* infections is on the rise due to a growing proportion of the population with weakened immune systems and increasing numbers of strains and species that are tolerant and/or resistant to antifungals (2, 6-9). Most *Candida* infections are caused by *C. albicans* and as much as 7% of isolates of this species are reportedly resistant to drugs (10, 11). Growing incidences of therapeutic failure in *C. albicans* and increasing observations of drug resistant strains of this

species and others like *Candida auris* and *Candida glabrata* are an impending public health crisis (9, 10, 12).

The emergence and expansion of drug-resistant *Candida* species are gradually eroding the potency of the current repertoire of antifungals (e.g., azoles, polyenes, echinocandins) used to treat invasive infections (10, 13). New antifungals are desperately needed, but drug discovery efforts are complicated by the phylogenetic conservation of druggable proteins and pathways in fungi and humans. Indeed, the small number of clinically used antifungals having good safety profiles critically perturb phenomena that are unique to fungi. A class of drugs having desirable selectivity and safety profiles are the azoles (14) and the prototypical member of this class of drugs is fluconazole (FLC) (8, 13-18). Azoles are fungistatic agents that act by inhibiting cytochrome P-450DM which catalyzes the conversion of lanosterol to ergosterol, an essential component of the fungal plasma membrane (19). Unfortunately, the azoles are also illustrative examples of how pathogenic fungi can become tolerant and resistant to antifungals. Azole resistance is commonly associated with genetic changes directly impacting drug action, including mutations in the drug target, overexpression of genes encoding efflux pumps, and/or increased copy numbers of beneficial alleles (13, 17, 18, 20). Tolerance to azoles is ascribed to intrinsic heterogeneity in fungal populations and is mediated by multiple stress response pathways (8, 15). The small number of drug targets that are unique to fungi and the intrinsic fungal tolerance and resistance to existing drugs make the development of new antifungals a challenging endeavor.

An alternative to developing novel antifungals is identifying compounds that can restore drug susceptibility in pathogenic fungi. Several reports describe molecules that potentiate azole activity against drug-resistant fungi. For instance, a chemical screen using the *Cryptococcus neoformans* overlap[2] method (O2M) led to the identification of dicyclomine,

sertraline, proadifen and chloroquine as azole potentiators (21). Similarly, inhibitors of Hsp90 and calcineurin were reported to suppress resistance and tolerance to FLC and combinations of the inhibitors with FLC were fungicidal (22-28). In another study, potentiation of FLC activity against *C. albicans* and *C. glabrata* by inhibitors of vesicular trafficking was described (29). Inspired by reports of azole potentiation, we performed a screen of an in-house collection of compounds in search of molecules that could restore FLC susceptibility to resistant and tolerant isolates of *C. albicans*. Here, we report the discovery and characterization of novel 1,4-benzodiazepines (1,4-BZDs) that restore azole activity against resistant and tolerant strains of *C. albicans*. The potentiation was synergistic and led to 100-1000-fold enhancement of FLC activity, higher than that of previously reported potentiators (21, 29). The potentiation was accompanied by a remarkable change in antifungal activity. Specifically, while FLC alone is fungistatic, combinations of the drug with 1,4-BZDs were fungicidal. The potentiation was of further interest because the 1,4-BZDs do not have intrinsic antifungal activity yet inhibit filamentation in *C. albicans.* Importantly, combinations of FLC and 1,4-BZDs significantly increased host survival in an *in vivo G. mellonella* model of fungal infection.

RESULTS

Discovery of potentiators of FLC activity. To identify compounds that potentiate FLC activity against drug-resistant and tolerant *C. albicans* strains, we screened an unbiased and structurally diverse library of ~100 compounds that had been synthesized in our laboratories. We included sortin2, dicyclomine, sertraline, proadifen and chloroquine as positive controls in our screen, owing to their previously reported azole potentiating activities (Fig. 1A) (21, 29). Careful consideration was also given to the *C. albicans* strains tested in the screen. We selected isolates with different FLC resistance/tolerance levels and from

diverse genetic backgrounds; specifically, the FLC-susceptible (yet tolerant) strain SC5314 [Clade 1, (30)], and the FLC-resistant strains SP-945 [Clade 3, (17, 31)] and P60002 [Clade SA, (30)] (Fig. 2A).

To identify compounds that can potentiate FLC, we utilized a FLC disk diffusion assay in which changes in both drug susceptibility and tolerance were assessed after 48 h growth on solid media supplemented with compounds in the library (100 μM) (32). Susceptibility was quantified by the clearance of fungal growth on solid media around a paper disk impregnated with azole at 50% and 20% growth inhibition (RAD_{50} and RAD_{20}, respectively, Fig. 2B) (32). On the other hand, tolerance was assessed using the fraction of growth inside the area of drug inhibition at 20% growth inhibition after 48 h (FoG_{20}, Fig. 2B). In combination with FLC, potentiators were expected to effect larger inhibition zones and/or decreased FoG_{20} levels relative to those observed when FLC was administered alone (Fig. 2C). In parallel, it was possible to determine whether the combination of FLC and screened compounds was fungistatic or fungicidal by replacing the FLC disk with a glucose disk and by measuring RAD_{50}, RAD_{20} and FoG_{20} following an additional 48 h growth period (Fig. 2C).

We were intrigued that several molecules that potentiated FLC activity against all three *C. albicans* strains tested were 1,4-BZDs. The 1,4-BZD core is a privileged scaffold in pharmacology and drug discovery having features that favor protein binding, including a semi-rigid scaffold, intermediate lipophilicity, and a combination of hydrogen bond donors and acceptors. This scaffold is found in several FDA approved drugs (33-35) and continues to be exploited in drug discovery efforts (36-42). The seven identified hits in the screen were among a group of twenty-six unique 1,4-BZDs in the library that differed by substitution patterns and the presence of either secondary or tertiary amide moieties (Fig. 1B). Each of the compounds was the product of a diversity-oriented synthetic route. The first building

blocks in the synthetic scheme were substituted diaryl ketoacetamides that were derived from substituted phenylacetamides (1a, Fig. S1) in a palladium mediated C-H activation. Acid-promoted N-deacetylation of those intermediates yielded diaryl aminoketones (2a) (43) that were elaborated into 1,4-BZDs having either secondary (3a) or tertiary amide moieties (4a). The former (3a) were accessed via a sequence of amidation followed by cyclization via reductive amination; the latter (4a) were prepared via a tandem Ugi-four component reaction and cyclization via reductive amination. All the advanced intermediates were elaborated into the collection of twenty-six 1,4-BZDs via acylations or reductive aminations (5a, 6a, 7a, Fig. S1). Interestingly, the seven screening hits (PA90, PA146, PA149, PA156, PA158, PA159 and PA162) restored FLC susceptibility and suppressed FLC tolerance in both resistant and tolerant *Candida* strains. Indeed, RAD_{50} values increased 2.2 to 387-fold and the RAD_{20} values increased 1.4 to 2.4-fold across the three strains for the seven 1,4-BZDs (Fig. 3A and S2A). Importantly, these compounds showed significant effects on FLC tolerance, with FoG_{20} levels decreasing 2.9 to 4.4-fold across the three strains and most of the compounds completely clearing tolerance (Fig. 3B and S2B). The capacity of the seven 1,4-BZDs to potentiate FLC against *C. albicans* strains with different resistance and tolerance levels was striking because previously reported FLC potentiators had strain specific effects. For example, proadifen only potentiated FLC against P60002 and sertraline potentiated FLC against SP-945, while showing reduced activity against other isolates (Fig. S2A-B). Additionally, the 1,4-BZDs exhibited greater potency than the previously reported potentiators in our experiments (Fig. S2A-B).

From the perspective of assessing structure activity-relationships, it was fortuitous that seven of the potentiators were among twenty-six 1,4-BZDs in our compound collection. Initially, we noted that most of the potentiators were 1,4-BZDs having secondary amides

(PA90, PA146, PA149, PA156, PA158, PA159); whereas only a single compound had a tertiary amide (PA162). Aside the secondary and tertiary amide distinction, there were other clear structural correlates for potentiation activity. For example, the potentiating compounds had large halogen substituents at the 7-position of the fused benzo moiety of the 1,4-BZD core. More specifically, compounds having bromine or chlorine substituents were active, whereas those having a fluorine or a hydrogen atom at the 7-position were less active. It was also interesting that the potentiating compounds, except for PA90, had halogen substituents on the exocyclic phenyl moiety. Fluorine or chlorine substituents at the 3- and/or 4-position of the exocyclic phenyl moiety were superior potentiators. Finally, all the potentiating compounds had a methylene 2-thiazole at N-4 of the 1,4-BZD core structure. This was critical as compounds having aliphatic or other aromatic substituents in the same N-4 position of the 1,4-BZD core did not potentiate FLC activity. Taken together, these observations indicate that a class of 1,4-BZDs (with 7-Br/7-Cl substituted benzo groups, 3 and/or 4 halogen substituted exocyclic phenyl and N-methylenethiazyl group) can significantly potentiate the activity of FLC against azole-resistant *C. albicans* strains.

1,4-BZDs are cidal in combination with FLC. The apparent potentiation of FLC activity by the 1,4-BZDs raised questions about the manner of growth inhibition. Specifically, we wanted to determine if the combinations were fungistatic (as is the case of FLC alone) or fungicidal. Thus, after growth on FLC with 1,4-BZDs, the FLC disk was replaced with a glucose disk, and RAD_{50}, RAD_{20} and FoG_{20} were measured again after 48 h of growth (Fig. 2C). Growth rebound in the initial zone of FLC inhibition upon removal of the antifungal was a marker of stasis, whereas the lack of growth indicated cidality. We found that growth on glucose disks resulted in modest differences in RAD_{50}, RAD_{20} and FoG_{20} values across the

seven 1,4-BZDs (Fig. 3A-B and S2C). This contrasted with results observed with previously reported potentiators, which elicited mostly fungistatic effects (Fig. S2A-B).

1,4-BZDs are synergistic with FLC against resistant and tolerant strains. After identification of seven 1,4-BZDs (PA90, PA146, PA149, PA156, PA158, PA159 and PA162) that potentiate FLC activity against *C. albicans*, we sought to define whether the compounds were acting additively or synergistically with the drug. Accordingly, we used the standard checkerboard assay in liquid growth media for assessing the mode of potentiation (21). In these assays, we measured the influence of 1,4-BZDs on both FLC susceptibility (MIC_{50} and MIC_{90}) and FLC tolerance (supra-MIC growth (15), SMG) starting at 128 µg/mL for FLC and 100 µM for the 1,4-BZDs in 2-fold serial dilutions. Sortin2 was included as a control in these experiments (29). These assays revealed significant FLC susceptibility restoration with the two resistant *C. albicans* isolates (SP-945, P60002) and FLC potentiation with the tolerant isolate (SC5314, Fig. 3C-D and S3A). PA149, PA158 and PA162 effected the largest changes in susceptibility (MIC_{90}) and tolerance across the 3 strains (SMG, Fig. 3C-D). In fact, combinations of FLC with 6.25-25 µM of these 1,4-BZDs lowered FLC MIC_{50}s 100 to 1000-fold (Fig. 3C and S3A). In contrast, sortin2 showed minimal FLC potentiation across strains, with significant effects observed only for SC5314 (drug-tolerant) at 25 µM (MIC_{90}, Fig. 3C and S3A). For azole tolerance, the strongest potentiators were PA149, PA156, PA158 and PA162 (Fig. 3D).

For all seven 1,4-BZDs, we calculated fractional inhibitory concentration indices (FICIs) at both 50% and 90% inhibition levels (Fig. 3E and S3B) to determine if they were acting additively or synergistically with FLC. For most interactions examined, $FICI_{90}$ scores were <0.5 against both drug-resistant and drug-tolerant strains, indicating synergistic

interactions between FLC and 1,4-BZDs. Synergies were most pronounced when the MIC_{90} was measured for strains SP-945 and SC5314 (Fig. 3E). For P60002, owing to its very high resistance levels (MIC_{50} >256 µg/ml FLC), synergistic interactions were most obvious at 50% inhibition ($FICI_{50}$, Fig. S3B). Overall, these assays revealed that FLC potentiation by the 1,4-BZDs is synergistic and that PA149, PA158 and PA162 were particularly potent at restoring FLC susceptibility to drug-resistant and drug-tolerant *C. albicans* strains.

1,4-BZDs are not toxic to *C. albicans* but inhibit filamentation. Negative controls (those lacking FLC) in the checkerboard assays indicated that the potentiating 1,4-BZDs alone did not have any inherent antifungal activity. To further explore these observations, we examined the influence of the potentiating 1,4-BZDs alone on fungal growth using drug-tolerant (SC5314) and drug-resistant (SP-945 and P60002) strains of *C. albicans*. Specifically, we monitored cell growth in liquid media supplemented with 1,4-BZDs at both 30 °C and 37 °C for 24 h. Sortin2 (29) was also included as a control in this experiment. We found that *C. albicans* growth was not affected by either sortin2 or any of the PA90, PA146, PA156, PA158 or PA162 compounds tested, even at the highest concentrations used in FLC restoration/potentiation assays (100 µM, Fig. 4A). Calculation of doubling times in the presence of 1,4-BZDs revealed no significant differences relative to the no drug condition across the tested compounds (Fig. 4B). The observations recapitulated those in the disk diffusion assays, in which the outer edges of the agar plates containing 1,4-BZDs showed no inhibition of *C. albicans* growth relative to regions close to the FLC disk (Fig. S2C) and point to minimal fungistatic or fungicidal effects of 1,4-BZDs in the absence of FLC.

The absence of toxicity for the 1,4-BZDs did not rule out the possibility that the compounds affected the physiology of *C. albicans*. In this regard, an important feature of

C. albicans is that it can transition to a filamentous morphology, which impacts its pathogenicity and commensalism (44-46). Accordingly, we used microscopy to assess the influence of the compounds on fungal cell morphology. SC5314, which is a highly filamentous strain (30), exhibited extensive filamentation, with ~89% of the population growing as hyphae or pseudohyphae following 2 h induction in liquid media at 37 °C (elongated cells, Fig. 5A-B). The other strains were less filamentous; only ~40% of P60002 and ~6% of SP-945 cells were filamenting under these conditions (Fig. 5A-B). We quantified cell morphologies of the *C. albicans* strains in the presence of two 1,4-BZDs, PA158 or PA162, which were selected due to their high potency and divergent chemotypes (Fig. 1B). Interestingly, treatment with 1,4-BZDs (at 100 µM) significantly reduced the number of hyphal and pseudohyphal cells for all *Candida* strains (Fig. 5A-B). In contrast, treatment with FLC alone (10 µg/mL) modestly affected filamentation, while a combination of 1,4-BZD/FLC (10 µg/mL FLC, 100 µM 1,4-BZDs) resulted in similar filamentation levels as those observed when the strains were treated with 1,4-BZDs alone (Fig. 5A-B). Because filamentation is important for *C. albicans* pathogenicity (45, 47) and its inhibition has emerged as a strategy for suppressing virulence (48-50), these observations suggest that the 1,4-BZDs could have utility beyond azole potentiation.

1,4-BZDs show restoration/potentiation activity in several *Candida* species. To gain further insights into FLC potentiation, we assessed the capacity of the 1,4-BZDs to potentiate FLC activity against phylogenetically diverse *Candida* species and more distantly related yeast, including *Candida dubiliniensis, Candida tropicalis, Candida parapsilosis, Candida metapsilosis, Candida orthopsilosis, Candida auris, Candida duobushaemulonii, Candida haemulonii, Candida krusei, Candida lusitaniae, Candida glabrata, Kodameae*

ohmeri and *Saccharomyces cerevisiae*. Initially, we determined the baseline FLC susceptibilities of isolates of these species in liquid growth media. Twenty-four of the 40 isolates examined had MIC_{50}s greater than 4 µg/mL, being classified as FLC-resistant by current MIC clinical breakpoints (except for *C. glabrata* where this breakpoint is 16 µg/mL FLC, (51)) (noted with R, Fig. 6A). Twenty-two of the 40 isolates had baseline SMG levels greater than or equal to 0.5 indicating that the isolates were tolerant to FLC (noted with T, Fig. 6B). Considering these parameters, we assessed the capacity of the 1,4-BZDs (PA90, PA149, PA156, PA158 and PA162) to potentiate FLC activity against the isolates at 100 µM. The MIC_{50} and MIC_{90} levels were quantified after 24 h and tolerance levels were determined after 48 h of growth. The assays revealed that selected 1,4-BZDs were able to potentiate FLC against isolates of *C. dubliniensis, C. tropicalis, C. haemulonii, C. duobushaemulonii*, *K. ohmeri*, *C. glabrata* and *S. cerevisiae* (Fig. 6A-B). In contrast, none of the 1,4-BZDs significantly potentiated FLC activity against *C. auris*, *C. krusei, C. lusitaniae, C. parapsilosis, C. metapsilosis,* and *C. orthopsilosis* (Fig. 6A-B). Interestingly, potentiation activities correlated with the phylogenetic relatedness of these species to *C. albicans*. The 1,4-BZDs displayed higher degrees of FLC potentiation against close relatives of *C. albicans* (*C. dubliniensis* and *C. tropicalis*) than against more phylogenetically distant species (e.g., *C. auris*) (Fig. 6C).

1,4-BZDs exclusively potentiate the azole class of antifungal drugs. Due to the synergistic potentiation of FLC activity by the 1,4-BZDs, we queried the specificity of the phenomenon by determining if the compounds could potentiate the activities of other antifungal agents. We explored the capacity of PA149, PA156, PA158, PA159 and PA162 (100 µM) to potentiate other azole drugs, including itraconazole (ITC), ketoconazole (KCA),

posaconazole (POS) and voriconazole (VOR) in disk diffusion assays with *C. albicans* strains SC5314 and P60002. The 1,4-BZDs tested restored the susceptibility of the resistant isolate P60002 (Fig. 7A) and suppressed the tolerance of SC5314 (Fig. 7B). Thus, azole/potentiator combinations led to increased susceptibility (higher RAD_{50} and RAD_{20}, Fig. 7A) and decreased tolerance (lower FoG_{20}, Fig. 7B). Again, the 1,4-BZDs compounds outperformed sortin2 which showed minimal potentiation in combination with other azoles.

Three of the potentiating 1,4-BZDs (PA90, PA146 and PA162) were also tested for their capacity to potentiate non-azole antifungals, including flucytosine (AFY), griseofulvin (AGF), amphotericin B (AMB), caspofungin (CAS) and nystatin (NY). These drugs have structures distinct from those of the azoles and do not target ergosterol biosynthesis. Their mechanisms of action include inhibition of DNA synthesis (AFY), perturbation of the fungal cell membrane (AMB, NY), disruption of cell wall β-1,3 glucan synthesis (CAS), and microtubule disassembly (AGF) (52, 53). In a marked difference from the azoles, we found that the 1,4-BZDs did not significantly potentiate the non-azole antifungal drugs (Fig. S4A-B). These results indicate that the potentiation effects of 1,4-BZDs are specific to azoles. Further mechanistic studies will be necessary to determine the molecular basis for the specificity of their potentiation.

Selected 1,4-BZDs affect intracellular accumulation of FLC in a drug-resistant strain. The apparent potentiation of FLC by 1,4-BZDs led us to inquire about the mechanism of the phenomenon. Given that the 1,4-BZDs only potentiate azoles, it is most likely that the 1,4-BZDs affect the action of azoles on P450DM or the ergosterol pathway. In one of multiple scenarios that could explain the potentiation, the 1,4-BZDs could directly or indirectly enhance the intracellular accumulation of azoles to an extent that they are active against

drug-resistant and drug-tolerant strains. To investigate the effects of 1,4-BZDs on intracellular azole levels, we performed experiments to quantify intracellular FLC concentrations using a previously reported fluorescent FLC analog (FLC-Cy5 at 1 µM) (54). FLC-Cy5 is easily visualized via fluorescence microscopy and has antifungal activity; however, it should be noted that some of its potency has been attributed to perturbation of targets other than P450DM (54). Consistent with a previous report, FLC-Cy5 displayed lower MIC_{50} values relative to FLC across the 3 tested *C. albicans* strains (Fig. S5A). Similarly, reduced tolerance (SMG) was observed with FLC-Cy5 (Fig. S5B). After recapitulating reported activities of the FLC-Cy5 probe, we assessed the capacity of 1,4-BZDs to potentiate the activity of FLC-Cy5. As a matter of convenience, five (PA90, PA146, PA158, PA159, PA162) of those potentiators were assessed for their capacity to potentiate FLC-Cy5. For reasons that are not clear, these compounds only potentiated the activity of FLC-Cy5 against P60002 (Fig. S5C). Curiously, the five 1,4-BZDs had minimal or no effects on the tolerance of *C. albicans* strains to FLC-Cy5 (SMG, Fig. S5D).

Having observed potentiation of FLC-Cy5 activity against the FLC-resistant strain P60002 by five different 1,4-BZDs, we measured the extent to which the compounds affected intracellular FLC-Cy5 levels. All five potentiators enhanced intracellular concentrations of FLC-Cy5 in P60002 by 2 to 3.8-fold (Figure 8A). With a single exception (i.e., PA162 and FLC-Cy5 against strain SC5314), none of the potentiators increased FLC-Cy5 accumulation in the other two strains. While the strain and compound-specific effects on FLC-Cy5 accumulation cannot be easily rationalized, our finding that the 1,4-BZDs enhanced FLC-Cy5 retention in the resistant strain P60002 suggests that FLC potentiation could be partially explained by enhancement of intracellular drug concentrations.

Mechanistically, intracellular accumulation of azoles in P60002 could occur via enhancement of uptake or inhibition of efflux. The latter phenomenon underlies the resistance of *Candida* to many drugs including the azoles (55-60). Indeed, multiple genes encoding efflux pumps have been associated with FLC resistance (58, 59, 61). The multiplicity of pumps complicated a genetic approach for investigating efflux thus we performed experiments wherein we directly compared the 1,4-BZDs with beauvericin, a promiscuous efflux inhibitor (55). We found that beauvericin enhanced FLC-Cy5 accumulation, similar to the effects of the five potentiators. However, upon treatment with beauvericin (1 μM), the intracellular levels of FLC-Cy5 were, on average, 1.4 to 2.5-fold higher than those observed with 1,4-BZD treatment (100 μM, Fig. 8A). Interestingly, the 1,4-BZDs do not fully phenocopy the efflux inhibitor beauvericin. Specifically, beauvericin also affects intracellular accumulation of rhodamine 6G (a known fluorescent efflux substrate, (60, 62)), whereas the 1,4-BZDs do not (Fig. 8B). This difference could be ascribed to the targeting of 1,4-BZDs to efflux pumps acting specifically on FLC-Cy5 but not on rhodamine 6G. Alternatively, the 1,4-BZDs may not perturb efflux. Indeed, some 1,4-BZDs potentiated FLC-Cy5 but did not increase the accumulation of the fluorescent FLC analog in the other two strains (SC5314, SP-945, Fig. S5A and 8A). In light of the conflicting observations, additional yet challenging experiments are needed to clarify the mode or modes of azole potentiation by the 1,4-BZDs.

1,4-BZD/FLC combinations improve *G. mellonella* survival during *C. albicans* systemic infection. Finally, we examined the impact of 1,4-BZD/FLC combinations on *G. mellonella* survival during systemic *C. albicans* infection. *G. mellonella* has been successfully utilized as a model for systemic infection for multiple pathogenic fungi. By extension, it is also frequently used for testing antifungal efficacy (63, 64). On these grounds,

G. mellonella larvae were systemically infected with SC5314, SP-945 or P60002 and treated with either a vehicle control (DMSO at matching volume), FLC, 1,4-BZDs, or 1,4-BZDs/FLC combinations (Fig. 9A-C). The larvae were then incubated at 37 °C and survival was monitored daily for 10 days. Control groups of larvae were used to assess the impact of these compounds on host survival in the absence of fungal infection (Fig. 9D). Treatment with FLC, sortin2 or 1,4-BZDs alone did not affect *Galleria* viability, indicating that these compounds are not overtly toxic to this organism (Fig. 9D). Experiments revealed that the different *C. albicans* isolates display distinct virulence dynamics and respond differently to FLC treatment. This was not surprising given the differences in genetic background, filamentation (Fig. 5), and azole susceptibilities (Fig. 2) of the three isolates. Infections by all strains resulted in significant host lethality, as evidenced by 3.5 ± 1.9% of larva survival at 10 days post infection (numbers represent a range across the three isolates). Treatment with FLC alone increased survival to 44.7 ± 9.4% of the infected larvae (Fig. 9A-C). Strikingly, treatment with combinations of FLC and potentiators significantly increased survival relative to FLC alone. Indeed, *Candida* infected larvae that were treated with FLC and either PA158 or PA162 survived at rates of 70.1 ± 16.2% and 68.8 ± 3.9%, respectively. These observations also stand in contrast to results observed when infected larvae were treated with a combination of FLC and sortin2. In this case, 47.2 ± 12.7% of the larvae survived and the sortin2 and FLC combination only improved the survival of larvae infected with SP-945 (Fig. 9B). It is also noteworthy that treatment of infected larvae with 1,4-BZDs alone significantly increased day 10 host survival rates (17.1 ± 11.3% with PA158 and 18.8 ± 5.5% with PA162 relative to 3.5 ± 1.9% with DMSO treatment). The enhanced survival rates effected by treatment with 1,4-BZDs as single agents could be explained by their capacity to inhibit parthenogenesis associated filamentation (Fig. 5) (45, 47). Taken together, these

observations indicate that the ability of 1,4-BZDs to potentiate FLC *in vitro* translates to *in vivo* infections.

DISCUSSION

Clinically, refractory invasive candidiasis is usually treated with single antifungal agents (11). The treatment of invasive candidiasis has been plagued by the emergence of drug resistant/tolerant species, a limited arsenal of antifungals and the lack of new antifungal molecules. The use of adjuvants that restore the activity of current antifungals could represent an effective therapeutic strategy. Here, we performed a small chemical screen in search of small molecules that could restore azole susceptibility to drug-tolerant and -resistant *Candida* species. We discovered seven unique 1,4-BZDs that potentiated FLC activity against azole-resistant and tolerant strains of *C. albicans.* Notably these 1,4-BZDs are structurally distinct from all the 1,4-BZD drugs like the anxiolytics and sedatives (e.g., diazepam, lorazepam, alprazolam, oxazepam, clonazepam). The compounds elicited up to 100-1000-fold potentiation of FLC activity (MIC_{50}) and cleared tolerance at concentrations of 6.25-25 µM. The 1,4-BZDs were able to restore the activity of a variety of other azoles (itraconazole, posaconazole, ketoconazole, voriconazole) but did not potentiate antifungal agents from other classes (caspofungin, amphotericin B, flucytosine, nystatin, griseofulvin). Importantly, while FLC is widely known as a fungistatic, the combination of FLC with the compounds was fungicidal. Checkerboard assays using 1,4-BZD/FLC combinations revealed that the compounds acted synergistically with FLC. The antifungal activity of the 1,4-BZDs and FLC combination was remarkable given that the 1,4-BZDs have no inherent antifungal activity when used alone. Testing the activity of these 1,4-BZDs on a broad panel of pathogenic and non-pathogenic yeast species revealed species-dependent potentiation, which was

associated with the phylogenetic relatedness of the different isolates tested. As the molecules were screened for activity in *C. albicans*, species more closely related to this fungus showed increased FLC potentiation (e.g., *C. tropicalis*, *C. dubliniensis*). This suggests that the genetic relatedness of the pathways targeted by 1,4-BZDs contributes to their efficacies in different species. Although we have not clarified the modes of potentiation of the 1,4-BZDs, our observations that the 1,4-BZDs phenocopy the intracellular accumulation of FLC-Cy5 by an efflux inhibitor in P60002 without influencing accumulation in other strains suggests that the mode of potentiation could depend on the genetic background of the isolate. Accordingly, we also observed that the 1,4-BZDs were most active in close phylogenetically related species to *Candida albicans* (Fig. 6). Additional studies will be required to delineate the pathways implicated in FLC potentiation by the 1,4-BZDs.

Our analyses revealed that combinations of 1,4-BZDs and FLC reduced *C. albicans* filamentation as well as improved survival in the *G. mellonella* model of systemic fungal infection. Although to a lesser degree, improved survival was also observed when 1,4-BZDs were used alone. Increased survival of *G. mellonella* could be mediated by the effects of the compounds on reducing filamentation, as this process is a key contributor to infection progression and lethality in this animal model (65). It remains to be established what filamentation pathways are modulated by 1,4-BZDs, either directly or indirectly. In addition, *in vivo* studies using models of mammalian fungal infection will be required to determine the efficacy of these molecules against *Candida* infection either alone or in combination with azoles.

Our observations support additional optimization of the different 1,4-BZD chemotypes as well as the molecular characterization and identification of the genes and pathways that underlie the effects of the 1,4-BZDs. Understanding the processes targeted by these

compounds on their own and in combination with azoles will provide new opportunities for the development of antifungal therapies.

MATERIALS AND METHODS

Synthesis of molecules. The 1,4-BZDs were prepared via a diversity-oriented synthetic scheme (Fig. S1). The scheme begins with substituted acetanilides (1): purchased or synthesized from aniline (66). We accessed the respective 2-aminoketones (2a) from the acetanilides through a combination C-H activation and subsequent acid-mediated removal of the acetyl- group (43, 67). The 2-aminoketones were converted to the substituted 5-phenyl-1,3,4,5-tetrahydro-2H-benzo[e][1,4]diazepin-2-one (3a, secondary amine) or the N-butyl-2-(2-oxo-5-phenyl-2,3,4,5-tetrahydro-1H-benzo[e][1,4]diazepin-1-yl)acetamide (4a) through a one-pot tandem reaction (involving amide formation for 3a and Ugi reaction for 4a), followed by intramolecular imine formation and reduction (68, 69). The secondary amine was further converted to the final products through acylation (acylation product 5a), or reductive amination (reductive amination products 6a and 7a) (70-73). The detailed procedures, characterization of 1,4-BZDs, and drugs used in this study are provided in the Supplemental Material.

Growth of fungal isolates. Strains used in this study are listed in Table 1. Fungal isolates were cultured overnight in 3 mL of liquid YPD (2% glucose, 2% bacto-peptone, 1% yeast extract, 2% dextrose) at 30 °C with shaking (200 rpm). Cell densities were measured using optical densities of culture dilutions (OD_{600}) in sterile water using a SPECTRAmax 250 Microplate Spectrophotometer. For growth curves, *C. albicans* cells were seeded in 96-well plates at a concentration of 2×10^5 cells/mL and grown in YPD at 30 °C or 37 °C with orbital

shaking for 24 h. Cell densities were measured every 15 min (OD_{600}) using a Biotek Epoch 2 plate reader and doubling times were calculated using the exponential growth phase of each curve.

Disk diffusion assays. For disk diffusion assays, *Candida* cultures were diluted to 1 x 10^6 cells/mL in sterile water and 100 μL of each diluted culture was spread on a YPD plate using glass beads. The plates were allowed to dry and a disk containing 25 μg FLC was placed in the center of each plate. The plates were incubated for 48 h at 30 °C, at which point they were photographed using a digital camera. To examine cidality, the FLC disk was replaced with a disk containing 8 mg of glucose and plates were grown for an additional 48 h. Disk images were analyzed using the R package *diskImageR* (32). The radius of inhibition (RAD) measures the distance (mm) from the center of the disk to the point where 20% or 50% reduction in growth occurs (RAD_{20} and RAD_{50}, respectively), quantifying the extent of the zone of inhibition around the FLC disk. The fraction of growth (FoG_{20}) calculates the area under the curve from the center of the disk to the 20% cutoff of inhibition. At least three independent disk assays were performed for each experiment.

MIC testing. MIC testing was performed using broth microdilution assays in 96-well plates. FLC was serially diluted (1 in 2) in liquid YPD to final concentrations of 0 - 128 μg/mL. Each well contained 125 μL liquid YPD volume with *C. albicans* cells at a concentration of 2 x 10^5 cells/mL. Plates were incubated at 30 °C with shaking (200 rpm) and cell densities (OD_{600}) were measured at 0, 24 and 48 h using a SPECTRAmax 250 Microplate Spectrophotometer. Plates were examined for contamination after each incubation period. MIC_{50}/MIC_{90} values were determined after 24 h growth by identifying the drug concentration

leading to less than or equal to 50%/90% growth relative to growth without drug (0 μg/mL FLC). Supra-MIC values, or SMG, were determined after 48 h growth by measuring the average growth levels above the MIC_{50} levels relative to growth without drug. At least 3 independent cell culture replicates were assayed for each experiment.

Checkerboard assays and FICI determination. For checkerboard assays 96 well plates were set up with drug combination containing FLC (0-128 µg/mL, X axis) and 1,4-BZDs (0-100 µM, Y axis) and serially diluted. Each well was seeded with *C. albicans* cells at a concentration of 2 x 10^5 cells/mL in 125 μL liquid YPD volume. Plates were incubated at 30 °C with shaking (200 rpm) and cell densities (OD_{600}) were measured at 0, 24 and 48 h using a SPECTRAmax 250 Microplate Spectrophotometer. Plates were examined for contamination after each incubation period. FLC MIC_{50}/MIC_{90} values for each row were determined after 24 h growth by identifying the drug concentration leading to less than or equal to 50%/90% growth relative to growth without drug (0 μg/mL FLC). Fractional inhibitory concentration indices ($FICI_{50}$ and $FICI_{90}$) were calculated as previously described (21) using FLC MIC_{50} and MIC_{90} levels, respectively. 3-4 independent assays were performed for each strain and each 1,4-BZD.

Flow cytometry. *C. albicans* cells were grown overnight in liquid YPD at 30 °C with shaking (200 rpm). Cultures were diluted 1:100 in 2-3 mL YPD medium and compounds were added to a final concentration of 10 µg/mL for FLC, 1 µM for FLC-Cy5, 10 µg/mL for Beauvericin, 1 µg/mL for Rhodamine 6G, and 100 µM for PA158 and PA162. Cells were incubated at 30 °C with shaking and harvested after 4 h, washed twice with sterile PBS and diluted to a density of ~10^6 cells/mL in PBS. Fluorescence was measured in 200 µL aliquots

of cell suspension and data were collected from 100,000 cells per sample using a Guava easyCyte 3rd generation and a BD FACSCelesta Cell Analyzer. Cell populations were gated by SSC/FSC to eliminate small debris particles. Experiments were performed with at least three biological and two technical replicates. Analyses were performed using FlowJo 10.8. Differences between conditions/treatments were evaluated using *t* tests, * $P < 0.05$.

Filamentation assays. For filamentation, *C. albicans* cells were grown overnight in liquid YPD at 30 °C with shaking, washed in PBS and resuspended in fresh YPD at a concentration of 10^5 cells/mL. 1 mL of cell suspension was added to 24-well plates and the plates were incubated at 37 °C without shaking for 2 h in the presence of DMSO (no drug), FLC alone (10 µg/mL), 1,4-BZDs (100 µM) or a combination of FLC (10 µg/mL) and 1,4-BZDs (100 µM). Wells were examined for distribution of cells on the surface of the wells and images of approximately 500-1000 cells were captured at a 40X magnification using a Zeiss AxioVision Rel. 4.8 microscope. Image analysis was performed using ImageJ to quantify the proportion of yeast, pseudohyphal, and hyphal cells present in each condition. Assays were performed with 4 biological and 2 technical replicates, differences between treatments were evaluated using *t* tests, * $P < 0.05$.

***In vivo* infections.** *G. mellonella* larvae were obtained from Vanderhorst Wholesale (Saint Marys, OH, USA) and the infection protocol was adapted from (15). Larvae were kept at 15 °C and used within 1 week of delivery. Larvae without signs of melanization and an average weight of 0.25 g were selected in groups of 12 larvae. *C. albicans* inoculums were prepared from cultures grown overnight at 30 °C in liquid YPD and washed twice with sterile PBS. Cell densities (OD_{600}) were measured using a SPECTRAmax 250 Microplate

Spectrophotometer and adjusted to 3×10^7 cells/mL in sterile PBS. Each larva was first injected with 3×10^5 *C. albicans* cells via the last left pro-leg using a 10 µL glass syringe and a 26S gauge needle (Hamilton, 80300). A second 10 µL injection with either FLC (20 µg/mL), 1,4-BZDs (50 µM), FLC (20 µg/mL) + 1,4-BZDs (50 µM), or sterile vehicle (DMSO) was done via the last right pro-leg 1.5–2 h post *C. albicans* infection. The inoculum size was confirmed by plating on YPD for colony forming units (CFUs). Infected and controls groups of larvae were maintained at 37 °C for 10 days and survival was checked daily. Larvae were recorded as dead if no movement was observed upon contact. Virulence assays were performed in 2-4 independent experiments ($n = 24$-48 total larvae per condition). Control groups of larvae included mock PBS injections (no *C. albicans*) followed by treatment with DMSO, FLC (20 µg/mL) or 1,4-BZDs (50 µM). No significant killing of larvae was observed in either of the control conditions. Statistical differences between larval groups were tested using Wilcoxon matched pairs signed rank tests, * $P < 0.01$.

Statistical analyses. Statistical analyses were carried out in GraphPad Prism 8 using two-tailed t-tests ($P < 0.05$) and Wilcoxon matched-pairs signed rank tests ($P < 0.01$).

ACKNOWLEDGEMENTS

We thank Kevin Carlson (Brown University) for support with flow cytometry experiments. We also thank Richard Bennett (Brown University), Brian LeBlanc (Brown University /RI Hospital), Joseph Bliss (Brown University /RI Hospital) and Arnaldo Colombo (Federal University of Sao Paolo) for the generous gift of strains. This work was supported by Brown University UTRA and SPRINT awards (TPM), NIH NIAID R21AI139592 (IVE),

CIFAR Azrieli Global Scholar Award (IVE) and Institut Pasteur (CG, IVE). JKS and PEA acknowledge generous funding from the Chan Zuckerberg Biohub and Brown University.

Tables

Table 1. Strains used in this study. For each species, the isolates are listed in the order in which they appear in Fig. 6.

Species	Name	Reference / Source
Candida albicans	SC5314	(74)
Candida albicans	SP-945 (Patient 15)	(17, 31)
Candida albicans	P60002	(30, 75)
Candida auris	CA01	CDC *Candida auris* panel
Candida auris	CA02	CDC *Candida auris* panel
Candida auris	CA03	CDC *Candida auris* panel
Candida auris	CA04	CDC *Candida auris* panel
Candida auris	CA05	CDC *Candida auris* panel
Candida auris	CA06	CDC *Candida auris* panel
Candida auris	CA07	CDC *Candida auris* panel
Candida auris	CA08	CDC *Candida auris* panel
Candida auris	CA09	CDC *Candida auris* panel
Candida auris	CA10	CDC *Candida auris* panel
Candida auris	CA21	CDC *Candida auris* panel
Candida auris	CA23	CDC *Candida auris* panel
Candida dubliniensis	SA100	Richard Bennett (Brown University)

Candida dubliniensis	4-7873A	Arnaldo Colombo (São Paulo-UNIFESP)
Candida dubliniensis	4-7873C	Arnaldo Colombo (São Paulo-UNIFESP)
Candida duobushaemulonii	CA11	CDC *Candida auris* panel
Candida duobushaemulonii	CA12	CDC *Candida auris* panel
Candida duobushaemulonii	CA14	CDC *Candida auris* panel
Candida glabrata	clinical isolate	Brian LeBlanc (RI Hospital)
Candida haemulonii	CA13	CDC *Candida auris* panel
Candida haemulonii	CA15	CDC *Candida auris* panel
Candida krusei	CA17	CDC *Candida auris* panel
Candida krusei	ATCC6258	Brian LeBlanc (RI Hospital)
Candida lusitaniae	CA18	CDC *Candida auris* panel
Candida metapsilosis	ATCC96143	Richard Bennett (Brown University)
Candida metapsilosis	CP43	Richard Bennett (Brown University)
Candida orthopsilosis	CP289	Richard Bennett (Brown University)
Candida orthopsilosis	CP331	Richard Bennett (Brown University)
Candida parapsilosis	R018-G3	Joseph Bliss (RI Hospital)
Candida parapsilosis	R029-O4	Joseph Bliss (RI Hospital)
Candida tropicalis	YBT44 ATC34139 ST-120	Richard Bennett (Brown University)
Candida tropicalis	YBT46 MYA-3404 T1	Richard Bennett (Brown University)

Candida tropicalis	ATCC13803	Brian LeBlanc (RI Hospital)
Kodameae ohmeri	CA16	CDC *Candida auris* panel
Saccharomyces cerevisiae	CA19	CDC *Candida auris* panel
Saccharomyces cerevisiae	CA20	CDC *Candida auris* panel
Saccharomyces cerevisiae	BY4741	Richard Bennett (Brown University)

Figure legends

Figure 1. Chemical structures of control compounds (A) and the set of twenty-six 1,4-BZDs (B) tested. The most active 1,4-BZDs are indicated in blue.

Figure 2. Screening strategy for 1,4-BZDs and control compounds. (A) FLC susceptibility profiles of *C. albicans* isolates SC5314, SP-945, and P60002 on disk diffusion assays, including their mean RAD_{50}, RAD_{20} and FoG_{20} levels. (B) A lawn of cells was plated on YPD and grown in the presence of a drug disk (FLC, 25 µg) for 48 h. The size of the radius at 50% and 20% growth inhibition (RAD_{50} and RAD_{20}, respectively) was measured as a proxy for susceptibility. The fraction of growth at 20% inhibition (FoG_{20}) was measured as a proxy for tolerance. Susceptibility and tolerance were determined using *diskImageR*. (C) Following 48 h of growth, the FLC disk was replaced with a glucose disk (G, 8 mg) and the plates were grown for another 48 h. For drug combinations, YPD plates contained 1,4-BZDs at 100 µM. Plates show example profiles of tolerant and resistant strains with FLC alone (left). Plates with FLC and potentiators (right) illustrate fungistatic or fungicidal effects of different drug combinations following additional growth on glucose disks.

Figure 3. Impact of the seven 1,4-BZD/FLC drug combinations on FLC susceptibility, tolerance and cell survival of *C. albicans*. Compounds were screened using FLC (25 µg) disk diffusion assays on YPD plates containing 100 µM 1,4-BZDs or the same volume of DMSO (vehicle). Panels indicate FLC susceptibility (RAD_{50} and RAD_{20}, A) and tolerance (FoG_{20}, B) following 48 h of growth. After 48 h, FLC disks were replaced with glucose disks (G, 8 mg), grown for an additional 48 h, and susceptibility and tolerance were quantified again. Heatmaps show average values for 3 or more biological replicates. (C-D) Checkerboard assays showing the impact of drug combinations of FLC (starting at 128 µg/mL) with the seven 1,4-BZDs (starting at 100 µM) on susceptibility (MIC_{90}, C) and tolerance (SMG, D) for *C. albicans* isolates SC5314, SP-945 and P60002. (E) $FICI_{90}$ scores for combinations of 1,4-BZDs and FLC based on 90% growth inhibition. Left-side table indicates the type of FLC-1,4-BZDs interaction based on the FICI score. FICI scores represent an average of 3-4 biological replicates.

Figure 4. Growth of isolates SC5314, SP-945 and P60002 in the presence of a subset of 1,4-BZDs. (A) Growth curves of *C. albicans* cells on YPD at 30 ºC and 37 ºC supplemented with DMSO, sortin2 or 1,4-BZDs (at 100 µM, sortin2 cultures have higher initial absorbance due to the orange color of the compound). (B) Relative doubling times of *C. albicans* cells in the presence of 1,4-BZDs, normalized to the no drug condition (DMSO). Growth curves and heatmaps show average values from 3 biological replicates.

Figure 5. Impact of drug combinations on *C. albicans* cell morphology. (A) Cell morphologies of strains SC5314, SP-945, P60002 treated with either DMSO, FLC (10 µg/mL), 1,4-BZDs (PA158 or PA162, 100 µM), or a combination of FLC (10 µg/mL) and 1,4-BZDs (100 µM).

Cells were incubated in YPD at 37 ºC for 2 h. Images show representative cells for the respective conditions, at 40X magnification. Scale bar, 10 µm. (B) The fraction of each morphology was quantified for at least 200 cells per condition with 4 biological replicates. Asterisks indicate significant differences relative to DMSO, *t* test, * $P < 0.05$.

Figure 6. Changes in susceptibility (MIC_{50} and MIC_{90}, A) and tolerance (SMG, B) of other yeast species using combinations of select 1,4-BZDs (100 µM) and FLC (from 0 to 256 µg/mL). R, FLC resistant isolates ($MIC_{50} \geq 16$ µg/mL for *C. glabrata* and $MIC_{50} \geq 4$ µg/mL for the rest of the species); T, FLC tolerant isolates (SMG ≥ 0.5). Heatmaps indicate average values from 3 biological replicates. (C) Phylogenetic relationships between different *Candida* species, adapted with permission from (76).

Figure 7. Changes in drug susceptibility (RAD_{50} and RAD_{20}, A) and tolerance (FoG_{20}, B) using combinations of a subset of 1,4-BZDs and other azole drugs. Compounds were screened using disk diffusion assays on YPD plates containing 1,4-BZDs (100 µM) or DMSO (no drug) and using disks of itraconazole (ITC, 50 µg), ketoconazole (KCA, 10 µg), posaconazole (POS, 5 µg), and voriconazole (VOR, 1 µg). Heatmaps indicate average values from 3 biological replicates.

Figure 8. Impact of 1,4-BZDs on intracellular FLC-Cy5 (A) and rhodamine 6G (B) accumulation. Fluorescence intensity levels were measured after 4 h incubation with FLC-Cy5 (1 µM) or rhodamine 6G (1 µg/mL) and treatment with either DMSO (no drug), 1,4-BZDs (100 µM), or beauvericin (10 µg/mL) for isolates SC5314, SP-945 and P60002. Values are

shown relative to corresponding DMSO controls. Asterisks indicate significant differences relative to DMSO, t test, * $P < 0.05$.

Figure 9. Impact of drug combinations on *G. mellonella* survival during systemic fungal infection. Larvae of *G. mellonella* were systemically infected with *C. albicans* isolates SC5314 (A), SP-945 (B), P60002 (C) and subsequently treated with either no drug (DMSO as vehicle), FLC (20 µg/mL), sortin2 (50 µM), 1,4-BZDs (PA158 or PA162, 50 µM), or a combination of FLC (20 µg/mL) and 1,4-BZDs (50 µM). Survival of larvae was monitored daily for 10 days for 2-4 groups of larvae with 12 larvae per group for each condition. Additional control groups of larvae were systemically injected with PBS and treated with either DMSO, FLC, sortin2, or 1,4-BZDs in the absence of fungal infection (D). Asterisks indicate significant differences for comparisons between treatments with single compounds (DMSO vs sortin2, DMSO vs FLC, DMSO vs PA158, DMSO vs PA162) or between drug combinations (FLC + DMSO, vs FLC + sortin2, FLC vs FLC + PA158, FLC vs FLC + PA162), colored according to the corresponding connecting curve, Wilcoxon matched-pairs signed rank test, * $P < 0.01$.

Supplemental Figure Legends

Figure S1. Synthetic scheme for accessing the different compounds tested. **a.** $Pd(OAc)_2$ 0.1eq., TBHP 4eq., TFA 0.3eq, substituted benzaldehyde or substituted benzyl alcohol 2eq., 40 ^{o}C, 16 h; **b.** excess Conc. HCl, EtOH, 75 ^{o}C, 16 h; **c.** Glycine N-carboxyanhydride (NCA) 1.3eq., TFA 2eq., Toluene (0.1 M), 65 ^{o}C, 30 min; **d.** Et_3N 2eq., 85 ^{o}C, 30 min; **e.** $NaBH_3CN$, AcOH, MeOH, room temperature, 16 h; **f.** n-butylisocyanide 1.1eq., formaldehyde 1eq., Boc-Glycine 1eq., MeOH, 24 h; **g.** TFA 2eq., Toluene, 70 ^{o}C; **h.** $NaBH_3CN$, AcOH, MeOH, 16 h;

i. R_1COCl, $NaHCO_3$, $CHCl_3$, 0 ^oC to room temperature, 12 h; **j** or **k** R_1CHO, $NaBH_3CN$, AcOH, MeOH, room temperature, 16 h.

Figure S2. Impact of 1,4-BZD/FLC drug combinations on FLC susceptibility, tolerance and cell survival of *C. albicans*. Compounds were screened using FLC (25 µg) disk diffusion assays on YPD plates containing 100 µM of compound or the same volume of DMSO (vehicle control). Panels indicate FLC susceptibility (RAD_{50} and RAD_{20}, A) and tolerance levels (FoG_{20}, B) following 48 h of growth. After 48 h, FLC disks were replaced with glucose disks (G, 8 mg), grown for an additional 48 h, and susceptibility and tolerance were quantified again. Heatmaps show average values for 3 or more biological replicates, arrows indicate the seven 1,4-BZD hits. (C) Representative images for FLC (at 48 h) and glucose (at 96 h) disk diffusion assays for strains SC5314, SP-945 and P60002 for potentiating 1,4-BZDs (used at 100 µM).

Figure S3. (A) Checkerboard assays showing the impact of drug combinations of FLC (starting at 128 µg/mL) with 1,4-BZDs (starting at 100 µM) on FLC susceptibility (MIC_{50}) for *C. albicans* isolates SC5314, SP-945 and P60002. (B) $FICI_{50}$ scores for combinations of the seven 1,4-BZDs and FLC based on 50% growth inhibition. Left-side table indicates the type of FLC-1,4-BZDs interaction based on the FICI score. FICI scores show an average of 3-4 biological replicates.

Figure S4. Changes in antifungal susceptibility (RAD_{50} and RAD_{20}, A) and tolerance (FoG_{20}, B) using combinations of a subset of 1,4-BZDs and non-azole antifungals. Compounds were screened using disk diffusion assays on YPD plates containing 1,4-BZDs (100 µM) or DMSO

(no drug) and using disks of flucytosine (AFY, 1 µg), griseofulvin (AGF, 10 µg), amphotericin B (AMB, 10 µg), caspofungin (CAS, 5 µg), and nystatin (NY, 100 IU). Heatmaps indicate average values from 3 biological replicates.

Figure S5. Comparison in antifungal susceptibility and tolerance (MIC_{50}, A and SMG, B) between FLC and FLC-Cy5 for isolates SC5314, SP-945 and P60002. (C-D) Changes in FLC-Cy5 susceptibility (MIC_{50}, C) and tolerance (SMG, D) for SC5314, SP-945 and P60002 when grown in the presence of drug combinations of FLC-Cy5 (0 to 10 µM) and 1,4-BZDs (used at 100 µM throughout). Heatmaps show average values from 3-4 biological replicates.

REFERENCES

1. Brown GD, Denning DW, Gow NA, Levitz SM, Netea MG, White TC. 2012. Hidden killers: human fungal infections. Sci Transl Med 4:165rv13.
2. Brown GD, Denning DW, Levitz SM. 2012. Tackling human fungal infections. Science 336:647.
3. Almeida F, Rodrigues ML, Coelho C. 2019. The Still Underestimated Problem of Fungal Diseases Worldwide. Front Microbiol 10:214.
4. Pappas PG, Lionakis MS, Arendrup MC, Ostrosky-Zeichner L, Kullberg BJ. 2018. Invasive candidiasis. Nat Rev Dis Primers 4:18026.
5. Kett DH, Azoulay E, Echeverria PM, Vincent JL, Extended Prevalence of Infection in ICUSGoI. 2011. *Candida* bloodstream infections in intensive care units: analysis of the extended prevalence of infection in intensive care unit study. Crit Care Med 39:665-70.

6. Bongomin F, Gago S, Oladele RO, Denning DW. 2017. Global and Multi-National Prevalence of Fungal Diseases-Estimate Precision. Journal of fungi (Basel, Switzerland) 3:57.
7. Roemer T, Krysan DJ. 2014. Antifungal drug development: challenges, unmet clinical needs, and new approaches. Cold Spring Harbor perspectives in medicine 4:a019703.
8. Berman J, Krysan DJ. 2020. Drug resistance and tolerance in fungi. Nat Rev Microbiol 18:319-331.
9. Arastehfar A, Lass-Florl C, Garcia-Rubio R, Daneshnia F, Ilkit M, Boekhout T, Gabaldon T, Perlin DS. 2020. The Quiet and Underappreciated Rise of Drug-Resistant Invasive Fungal Pathogens. J Fungi (Basel) 6.
10. Arastehfar A, Gabaldon T, Garcia-Rubio R, Jenks JD, Hoenigl M, Salzer HJF, Ilkit M, Lass-Florl C, Perlin DS. 2020. Drug-Resistant Fungi: An Emerging Challenge Threatening Our Limited Antifungal Armamentarium. Antibiotics (Basel) 9.
11. Pfaller MA, Diekema DJ, Turnidge JD, Castanheira M, Jones RN. 2019. Twenty Years of the SENTRY Antifungal Surveillance Program: Results for *Candida* Species From 1997-2016. Open Forum Infect Dis 6:S79-S94.
12. Forsberg K, Woodworth K, Walters M, Berkow EL, Jackson B, Chiller T, Vallabhaneni S. 2019. Candida auris: The recent emergence of a multidrug-resistant fungal pathogen. Med Mycol 57:1-12.
13. Robbins N, Caplan T, Cowen LE. 2017. Molecular Evolution of Antifungal Drug Resistance. Annu Rev Microbiol 71:753-775.
14. Fisher MC, Hawkins NJ, Sanglard D, Gurr SJ. 2018. Worldwide emergence of resistance to antifungal drugs challenges human health and food security. Science 360:739-742.

15. Rosenberg A, Ene IV, Bibi M, Zakin S, Segal ES, Ziv N, Dahan AM, Colombo AL, Bennett RJ, Berman J. 2018. Antifungal tolerance is a subpopulation effect distinct from resistance and is associated with persistent candidemia. Nat Commun 9:2470.
16. Lee Y, Puumala E, Robbins N, Cowen LE. 2021. Antifungal Drug Resistance: Molecular Mechanisms in *Candida albicans* and Beyond. Chem Rev 121:3390-3411.
17. Ford CB, Funt JM, Abbey D, Issi L, Guiducci C, Martinez DA, Delorey T, Li BY, White TC, Cuomo C, Rao RP, Berman J, Thompson DA, Regev A. 2015. The evolution of drug resistance in clinical isolates of *Candida albicans*. Elife 4:e00662.
18. Berkow EL, Lockhart SR. 2017. Fluconazole resistance in *Candida* species: a current perspective. Infection and drug resistance 10:237-245.
19. Hitchcock CA, Dickinson K, Brown SB, Evans EG, Adams DJ. 1990. Interaction of azole antifungal antibiotics with cytochrome P-450-dependent 14 alpha-sterol demethylase purified from *Candida albicans*. Biochem J 266:475-80.
20. Cowen LE, Sanglard D, Howard SJ, Rogers PD, Perlin DS. 2014. Mechanisms of Antifungal Drug Resistance. Cold Spring Harbor perspectives in medicine 5:a019752-a019752.
21. Wambaugh MA, Denham ST, Ayala M, Brammer B, Stonhill MA, Brown JCS. 2020. Synergistic and antagonistic drug interactions in the treatment of systemic fungal infections. eLife 9:e54160.
22. Cowen LE. 2013. The fungal Achilles' heel: targeting Hsp90 to cripple fungal pathogens. Current Opinion in Microbiology 16:377-384.
23. Cowen LE, Carpenter AE, Matangkasombut O, Fink GR, Lindquist S. 2006. Genetic architecture of Hsp90-dependent drug resistance. Eukaryotic cell 5:2184-2188.

24. Cowen LE, Lindquist S. 2005. Hsp90 Potentiates the Rapid Evolution of New Traits: Drug Resistance in Diverse Fungi. Science 309:2185.
25. Rosenberg A, Ene IV, Bibi M, Zakin S, Segal ES, Ziv N, Dahan AM, Colombo AL, Bennett RJ, Berman J. 2018. Antifungal tolerance is a subpopulation effect distinct from resistance and is associated with persistent candidemia. Nature Communications 9:2470.
26. Juvvadi PR, Lee SC, Heitman J, Steinbach WJ. 2017. Calcineurin in fungal virulence and drug resistance: Prospects for harnessing targeted inhibition of calcineurin for an antifungal therapeutic approach. Virulence 8:186-197.
27. Onyewu C, Wormley FL, Jr., Perfect JR, Heitman J. 2004. The calcineurin target, Crz1, functions in azole tolerance but is not required for virulence of *Candida albicans*. Infection and immunity 72:7330-7333.
28. Cruz MC, Goldstein AL, Blankenship JR, Del Poeta M, Davis D, Cardenas ME, Perfect JR, McCusker JH, Heitman J. 2002. Calcineurin is essential for survival during membrane stress in *Candida albicans*. EMBO J 21:546-59.
29. Demuyser L, Van Dyck K, Timmermans B, Van Dijck P. 2019. Inhibition of Vesicular Transport Influences Fungal Susceptibility to Fluconazole. Antimicrobial Agents and Chemotherapy 63:e01998-18.
30. Hirakawa MP, Martinez DA, Sakthikumar S, Anderson MZ, Berlin A, Gujja S, Zeng Q, Zisson E, Wang JM, Greenberg JM, Berman J, Bennett RJ, Cuomo CA. 2015. Genetic and phenotypic intra-species variation in *Candida albicans*. Genome Res 25:413-25.
31. Perea S, Lopez-Ribot JL, Kirkpatrick WR, McAtee RK, Santillan RA, Martinez M, Calabrese D, Sanglard D, Patterson TF. 2001. Prevalence of molecular mechanisms of resistance to azole antifungal agents in *Candida albicans* strains displaying high-level

fluconazole resistance isolated from human immunodeficiency virus-infected patients. Antimicrob Agents Chemother 45:2676-84.

32. Gerstein AC, Rosenberg A, Hecht I, Berman J. 2016. diskImageR: quantification of resistance and tolerance to antimicrobial drugs using disk diffusion assays. Microbiology (Reading, England) 162:1059-1068.
33. Calcaterra NE, Barrow JC. 2014. Classics in chemical neuroscience: diazepam (valium). ACS chemical neuroscience 5:253-260.
34. Ameer B, Greenblatt DJ. 1981. Lorazepam: A Review of its Clinical. Drugs 21:161-200.
35. Lawrence JM, Edwards JE, Briggs GS, Jones IH. 1974. A controlled clinical trial of a new antianxiety agent lorazepam (ativan). Medical Journal of Australia 2:660-661.
36. Buettelmann B, Ballard TM, Gasser R, Fischer H, Hernandez M-C, Knoflach F, Knust H, Stadler H, Thomas AW, Trube G. 2009. Imidazo[1,5-a][1,2,4]-triazolo[1,5-d][1,4]benzodiazepines as potent and highly selective GABAA alpha5 inverse agonists with potential for the treatment of cognitive dysfunction. Bioorganic & medicinal chemistry letters 19:5958-5961.
37. Eguchi M. 2004. Recent advances in selective opioid receptor agonists and antagonists. Medicinal Research Reviews 24:182-212.
38. Chapman J, Abbott E, Alber DG, Baxter RC, Bithell SK, Henderson EA, Carter MC, Chambers P, Chubb A, Cockerill GS, Collins PL, Dowdell VCL, Keegan SJ, Kelsey RD, Lockyer MJ, Luongo C, Najarro P, Pickles RJ, Simmonds M, Taylor D, Tyms S, Wilson LJ, Powell KL. 2007. RSV604, a novel inhibitor of respiratory syncytial virus replication. Antimicrobial agents and chemotherapy 51:3346-3353.
39. Ettari R, Micale N, Schirmeister T, Gelhaus C, Leippe M, Nizi E, Di Francesco ME, Grasso S, Zappalà M. 2009. Novel Peptidomimetics Containing a Vinyl Ester Moiety as

Highly Potent and Selective Falcipain-2 Inhibitors. Journal of Medicinal Chemistry 52:2157-2160.

40. Gavai AV, Quesnelle C, Norris D, Han W-C, Gill P, Shan W, Balog A, Chen K, Tebben A, Rampulla R, Wu D-R, Zhang Y, Mathur A, White R, Rose A, Wang H, Yang Z, Ranasinghe A, D'Arienzo C, Guarino V, Xiao L, Su C, Everlof G, Arora V, Shen DR, Cvijic ME, Menard K, Wen M-L, Meredith J, Trainor G, Lombardo LJ, Olson R, Baran PS, Hunt JT, Vite GD, Fischer BS, Westhouse RA, Lee FY. 2015. Discovery of Clinical Candidate BMS-906024: A Potent Pan-Notch Inhibitor for the Treatment of Leukemia and Solid Tumors. ACS Medicinal Chemistry Letters 6:523-527.
41. Tardibono LP, Miller MJ. 2009. Synthesis and Anticancer Activity of New Hydroxamic Acid Containing 1,4-Benzodiazepines. Organic Letters 11:1575-1578.
42. Liu J, Cheng AC, Tang HL, Medina JC. 2011. Benzodiazepinone Derivatives as CRTH2 Antagonists. ACS Medicinal Chemistry Letters 2:515-518.
43. Luo F, Yang J, Li Z, Xiang H, Zhou X. 2015. Palladium-Catalyzed C–H Bond Acylation of Acetanilides with Benzylic Alcohols under Aqueous Conditions. European Journal of Organic Chemistry 2015:2463-2469.
44. Witchley JN, Penumetcha P, Abon NV, Woolford CA, Mitchell AP, Noble SM. 2019. *Candida albicans* Morphogenesis Programs Control the Balance between Gut Commensalism and Invasive Infection. Cell Host Microbe 25:432-443 e6.
45. Noble SM, Gianetti BA, Witchley JN. 2017. *Candida albicans* cell-type switching and functional plasticity in the mammalian host. Nat Rev Microbiol 15:96-108.
46. Sudbery PE. 2011. Growth of *Candida albicans* hyphae. Nature reviews Microbiology 9:737-748.

47. Mayer FL, Wilson D, Hube B. 2013. *Candida albicans* pathogenicity mechanisms. Virulence 4:119-128.
48. Kadosh D. 2019. Regulatory mechanisms controlling morphology and pathogenesis in *Candida albicans*. Current Opinion in Microbiology 52:27-34.
49. Romo JA, Pierce CG, Chaturvedi AK, Lazzell AL, McHardy SF, Saville SP, Lopez-Ribot JL. 2017. Development of Anti-Virulence Approaches for Candidiasis via a Novel Series of Small-Molecule Inhibitors of *Candida albicans* Filamentation. mBio 8:e01991-17.
50. Vila T, Romo JA, Pierce CG, McHardy SF, Saville SP, Lopez-Ribot JL. 2017. Targeting *Candida albicans* filamentation for antifungal drug development. Virulence 8:150-158.
51. Arendrup MC, Friberg N, Mares M, Kahlmeter G, Meletiadis J, Guinea J, Subcommittee on Antifungal Susceptibility Testing of the EUCAST. 2020. How to interpret MICs of antifungal compounds according to the revised clinical breakpoints v. 10.0 European committee on antimicrobial susceptibility testing (EUCAST). Clin Microbiol Infect 26:1464-1472.
52. Odds FC, Brown AJ, Gow NA. 2003. Antifungal agents: mechanisms of action. Trends in microbiology 11:272-279.
53. Serhan G, Stack CM, Perrone GG, Morton CO. 2014. The polyene antifungals, amphotericin B and nystatin, cause cell death in *Saccharomyces cerevisiae* by a distinct mechanism to amphibian-derived antimicrobial peptides. Ann Clin Microbiol Antimicrob 13:18.
54. Benhamou RI, Bibi M, Steinbuch KB, Engel H, Levin M, Roichman Y, Berman J, Fridman M. 2017. Real-Time Imaging of the Azole Class of Antifungal Drugs in Live *Candida* Cells. ACS Chemical Biology 12:1769-1777.

55. Shekhar-Guturja T, Tebung WA, Mount H, Liu N, Köhler JR, Whiteway M, Cowen LE. 2016. Beauvericin Potentiates Azole Activity via Inhibition of Multidrug Efflux, Blocks *Candida albicans* Morphogenesis, and Is Effluxed via Yor1 and Circuitry Controlled by Zcf29. Antimicrobial Agents and Chemotherapy 60:7468.
56. Prasad R, Rawal MK. 2014. Efflux pump proteins in antifungal resistance. Frontiers in Pharmacology 5.
57. Prasad R, Gaur NA, Gaur M, Komath SS. 2006. Efflux Pumps in Drug Resistance of *Candida*. Infectious Disorders - Drug Targets 6:69-83.
58. Song M, Zhang M, Lu J, Xie F, Song J, Luan X, Hou X, Lou H, Chang W. Palmarumycin P3 Reverses Mrr1-Mediated Azole Resistance by Blocking the Efflux Pump Mdr1. Antimicrobial Agents and Chemotherapy 66:e02126-21.
59. Schuetzer-Muehlbauer M, Willinger B, Egner R, Ecker G, Kuchler K. 2003. Reversal of antifungal resistance mediated by ABC efflux pumps from *Candida albicans* functionally expressed in yeast. International Journal of Antimicrobial Agents 22:291-300.
60. Maesaki S, Marichal P, Bossche HV, Sanglard D, Kohno S. 1999. Rhodamine 6G efflux for the detection of *CDR1*-overexpressing azole-resistant *Candida albicans* strains. Journal of Antimicrobial Chemotherapy 44:27-31.
61. Mukherjee PK, Chandra J, Kuhn DM, Ghannoum MA. 2003. Mechanism of fluconazole resistance in *Candida albicans* biofilms: phase-specific role of efflux pumps and membrane sterols. Infection and immunity 71:4333-4340.
62. Whittle EE, Legood SW, Alav I, Dulyayangkul P, Overton TW, Blair JMA. 2019. Flow Cytometric Analysis of Efflux by Dye Accumulation. Frontiers in Microbiology 10:2319.
63. Arvanitis M, Glavis-Bloom J, Mylonakis E. 2013. Invertebrate models of fungal infection. Biochim Biophys Acta 1832:1378-83.

64. Li DD, Deng L, Hu GH, Zhao LX, Hu DD, Jiang YY, Wang Y. 2013. Using *Galleria mellonella-Candida albicans* infection model to evaluate antifungal agents. Biol Pharm Bull 36:1482-7.

65. Fuchs BB, Eby J, Nobile CJ, El Khoury JB, Mitchell AP, Mylonakis E. 2010. Role of filamentation in *Galleria mellonella* killing by *Candida albicans.* Microbes Infect 12:488-96.

66. Yamasaki R, Tanatani A, Azumaya I, Saito S, Yamaguchi K, Kagechika H. 2003. Amide Conformational Switching Induced by Protonation of Aromatic Substituent. Organic Letters 5:1265-1267.

67. Wang X, Ahn Y-M, Lentscher AG, Lister JS, Brothers RC, Kneen MM, Gerratana B, Boshoff HI, Dowd CS. 2017. Design, synthesis, and evaluation of substituted nicotinamide adenine dinucleotide (NAD+) synthetase inhibitors as potential antitubercular agents. Bioorganic & Medicinal Chemistry Letters 27:4426-4430.

68. Azuaje J, Pérez-Rubio JM, Yaziji V, El Maatougui A, González-Gomez JC, Sánchez-Pedregal VcM, Navarro-Vázquez A, Masaguer CF, Teijeira M, Sotelo E. 2015. Integrated Ugi-Based Assembly of Functionally, Skeletally, and Stereochemically Diverse 1,4-Benzodiazepin-2-ones. The Journal of Organic Chemistry 80:1533-1549.

69. Fier PS, Whittaker AM. 2017. An Atom-Economical Method To Prepare Enantiopure Benzodiazepines with N-Carboxyanhydrides. Organic Letters 19:1454-1457.

70. Pinsker A, Einsiedel J, Härterich S, Waibel R, Gmeiner P. 2011. A Highly Efficient Type I β-Turn Mimetic Simulating an Asx-Pro-Turn-Like Structure. Organic Letters 13:3502-3505.

71. Schepartz A. 1987. Hydrolysis of an amide in a carboxypeptidase model using cobalt(III) and bifunctional catalysts. Journal of the American Chemical Society 109:1814 - EOA.

72. Shi W. 2011. Effect of carbohydrate amino group modifications on the cytotoxicity of glycosylated 2-phenyl-benzo[b]thiophenes and 2-phenyl-benzo[b]furans. Bioorganic & medicinal chemistry letters 21:5107 - EOA.
73. Galley G. 2016. Discovery and Characterization of 2-Aminooxazolines as Highly Potent, Selective, and Orally Active TAAR1 Agonists. ACS medicinal chemistry letters 7:192 - EOA.
74. Maestrone G, Semar R. 1968. Establishment and treatment of cutaneous *Candida albicans* infection in the rabbit. Naturwissenschaften 55:87-8.
75. Wu W, Lockhart SR, Pujol C, Srikantha T, Soll DR. 2007. Heterozygosity of genes on the sex chromosome regulates *Candida albicans* virulence. Molecular microbiology 64:1587-1604.
76. Munoz JF, Gade L, Chow NA, Loparev VN, Juieng P, Berkow EL, Farrer RA, Litvintseva AP, Cuomo CA. 2018. Genomic insights into multidrug-resistance, mating and virulence in *Candida auris* and related emerging species. Nat Commun 9:5346.

Figure 1.

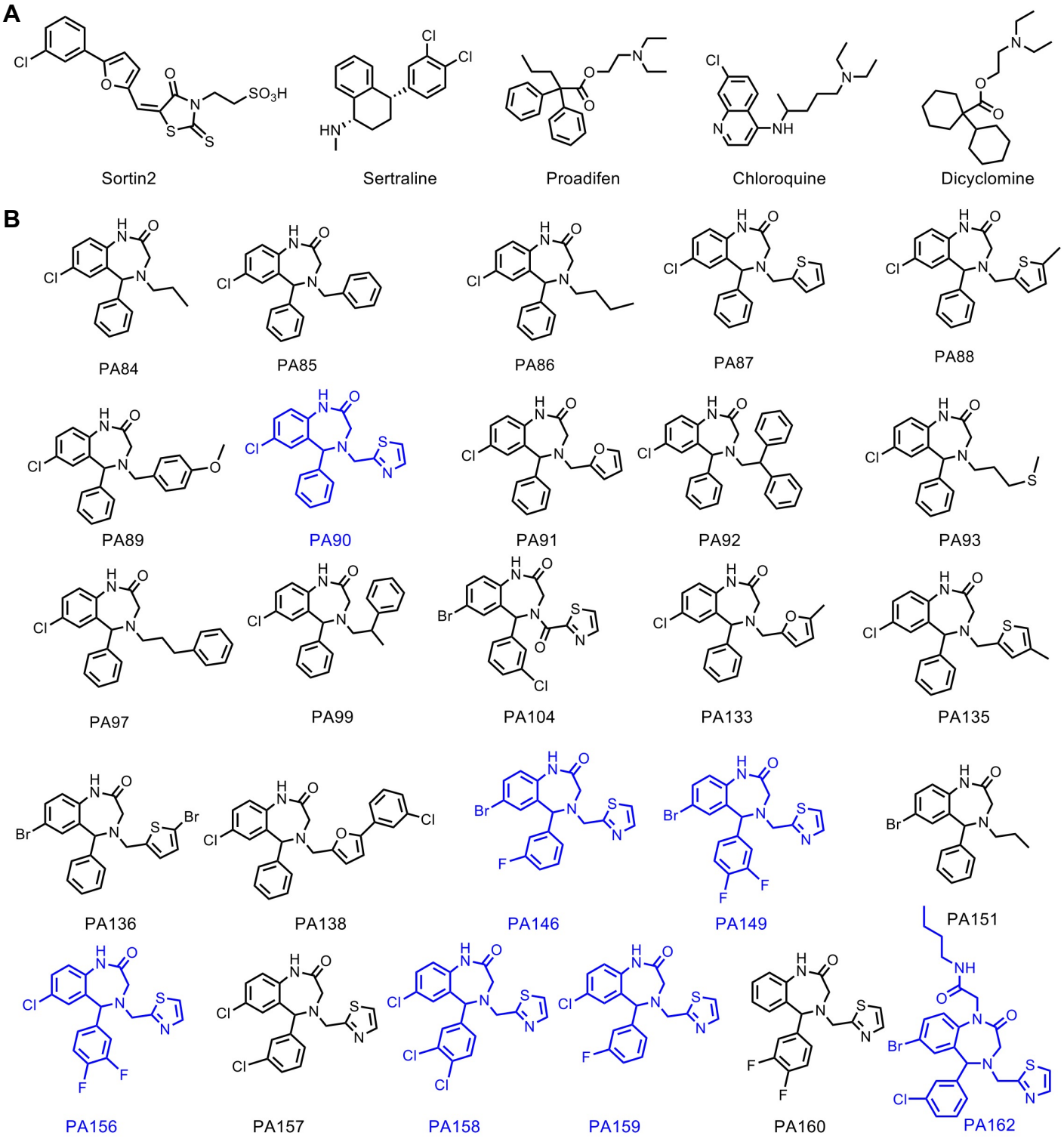
A
Sortin2
Sertraline
Proadifen
Chloroquine
Dicyclomine
B
PA84
PA85
PA86
PA87
PA88
PA89
PA90
PA91
PA92
PA93
PA97
PA99
PA104
PA133
PA135
PA136
PA138
PA146
PA149
PA151
PA156
PA157
PA158
PA159
PA160
PA162

Figure 2.

A

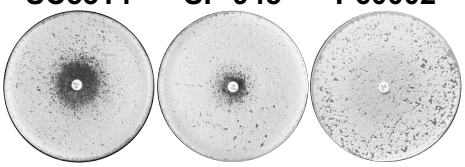

	SC5314	SP-945	P60002
	tolerant	resistant	resistant
RAD_{50}	7.9	3.9	0
RAD_{20}	13	5.6	10.6
FoG_{20}	0.53	0.5	0.93

B

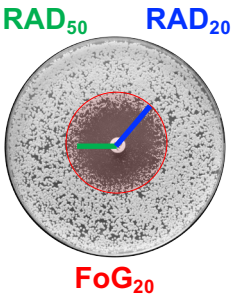

C

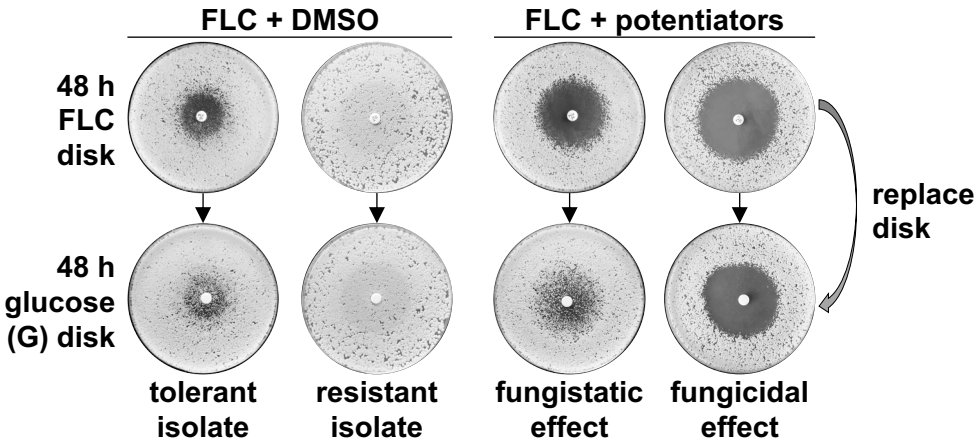

Figure 3.

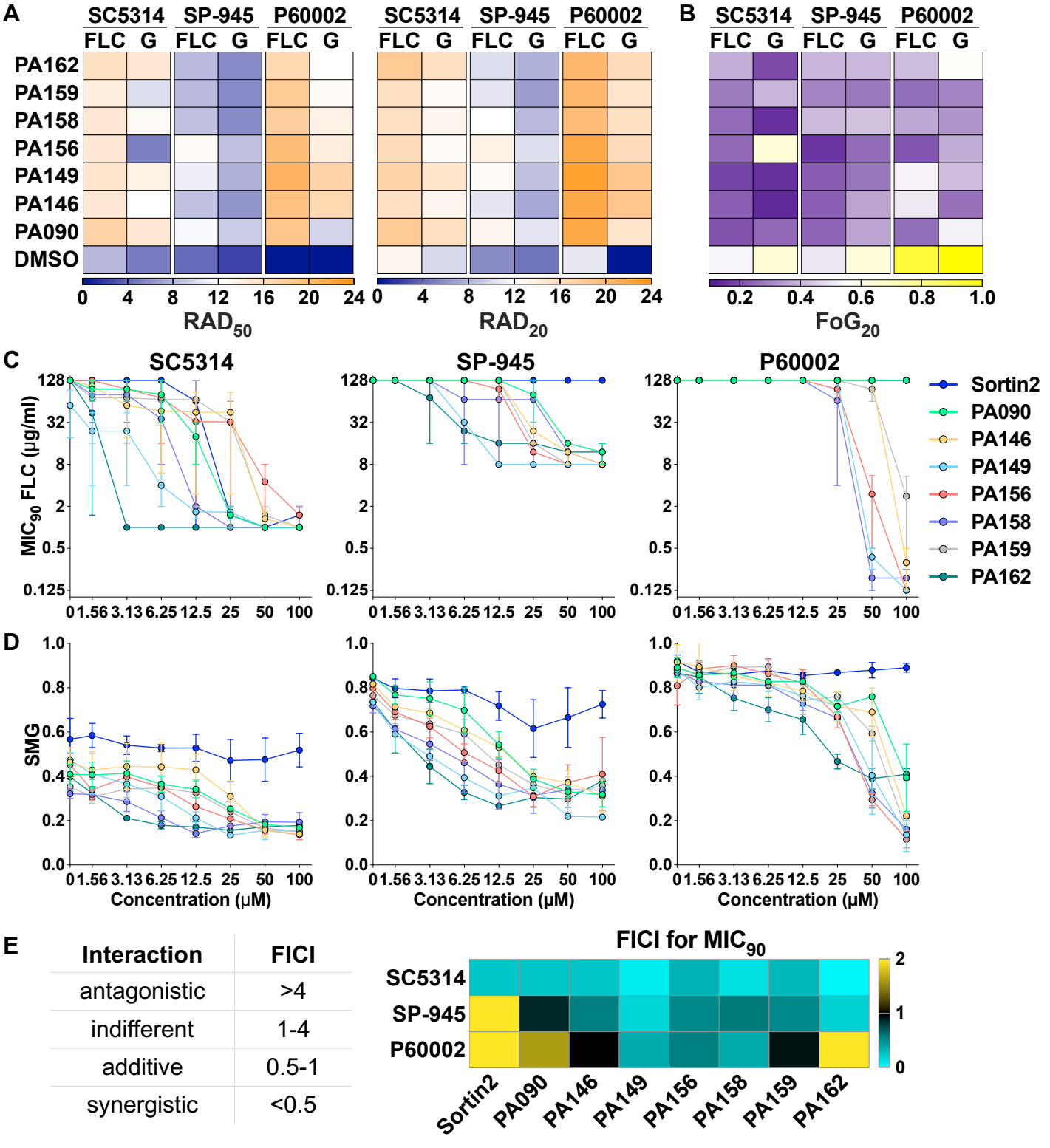

Interaction	FICI
antagonistic	>4
indifferent	1-4
additive	0.5-1
synergistic	<0.5

Figure 4.

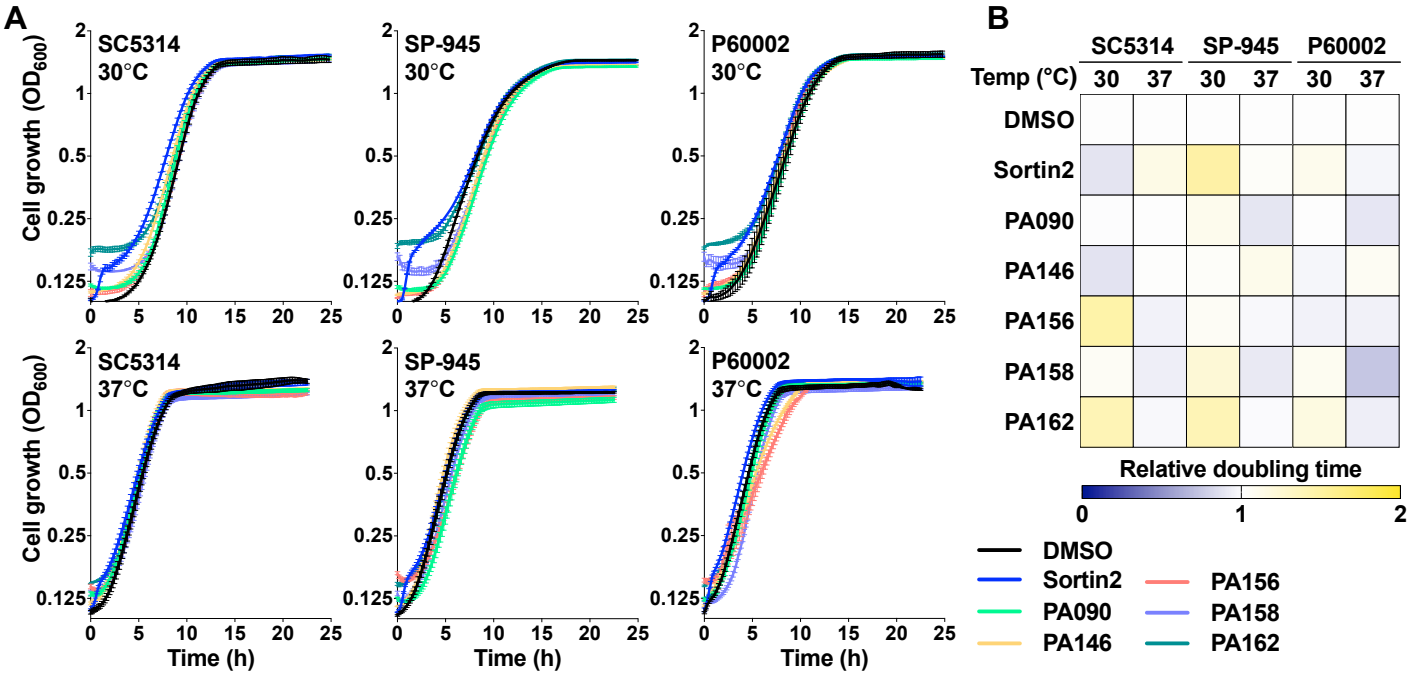
A
SC5314
30°C
SP-945
30°C
P60002
30°C
SC5314
37°C
SP-945
37°C
P60002
37°C
Cell growth (OD600)
Time (h)
B
SC5314
SP-945
P60002
Temp (°C)
30
37
DMSO
Sortin2
PA090
PA146
PA156
PA158
PA162
Relative doubling time
0
1
2
DMSO
Sortin2
PA090
PA146
PA156
PA158
PA162

Figure 5.

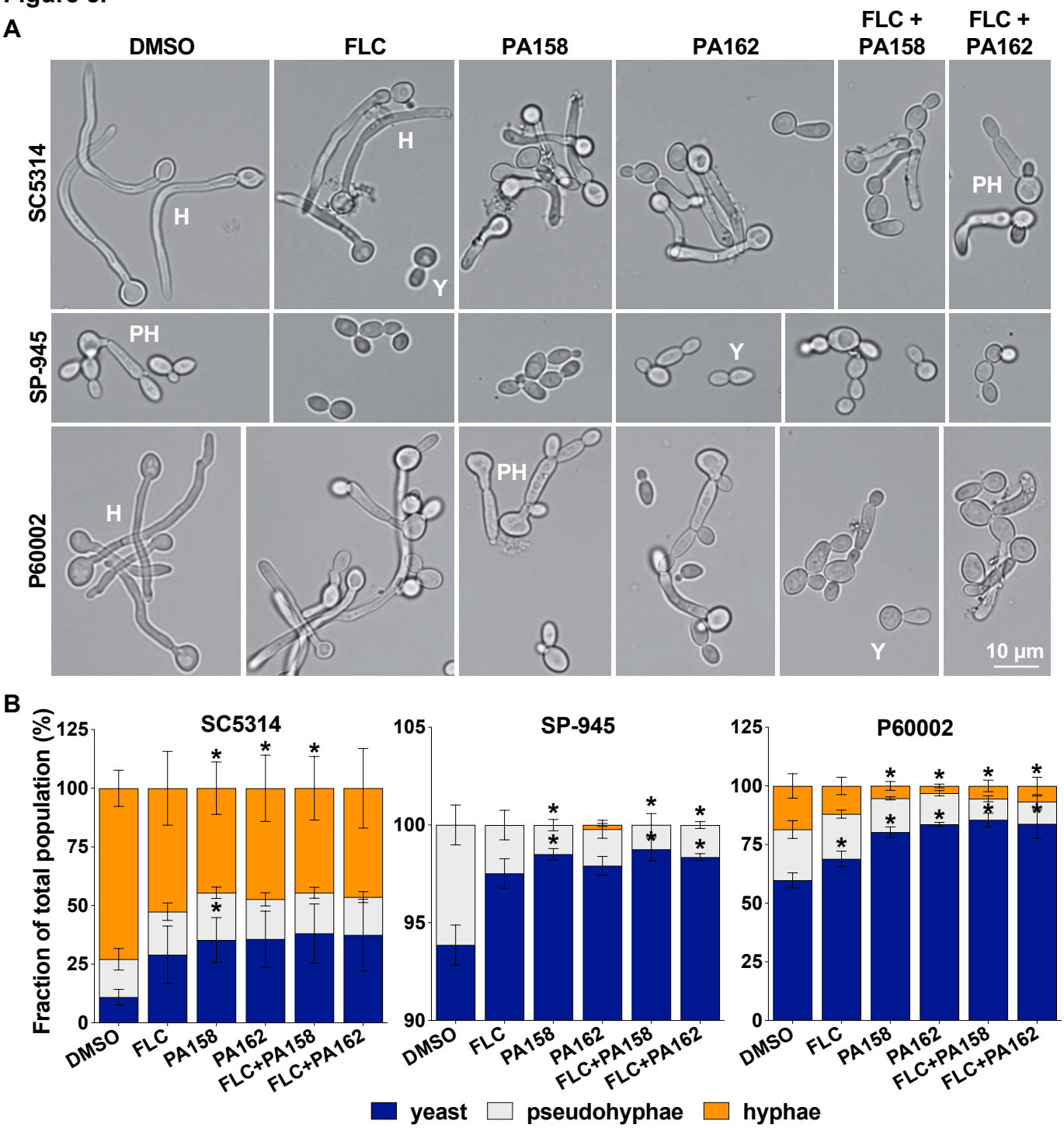
A
DMSO
FLC
PA158
PA162
FLC + PA158
FLC + PA162
SC5314
SP-945
P60002
H
Y
PH
10 µm
B
SC5314
SP-945
P60002
Fraction of total population (%)
DMSO
FLC
PA158
PA162
FLC+PA158
FLC+PA162
yeast
pseudohyphae
hyphae

Figure 6.

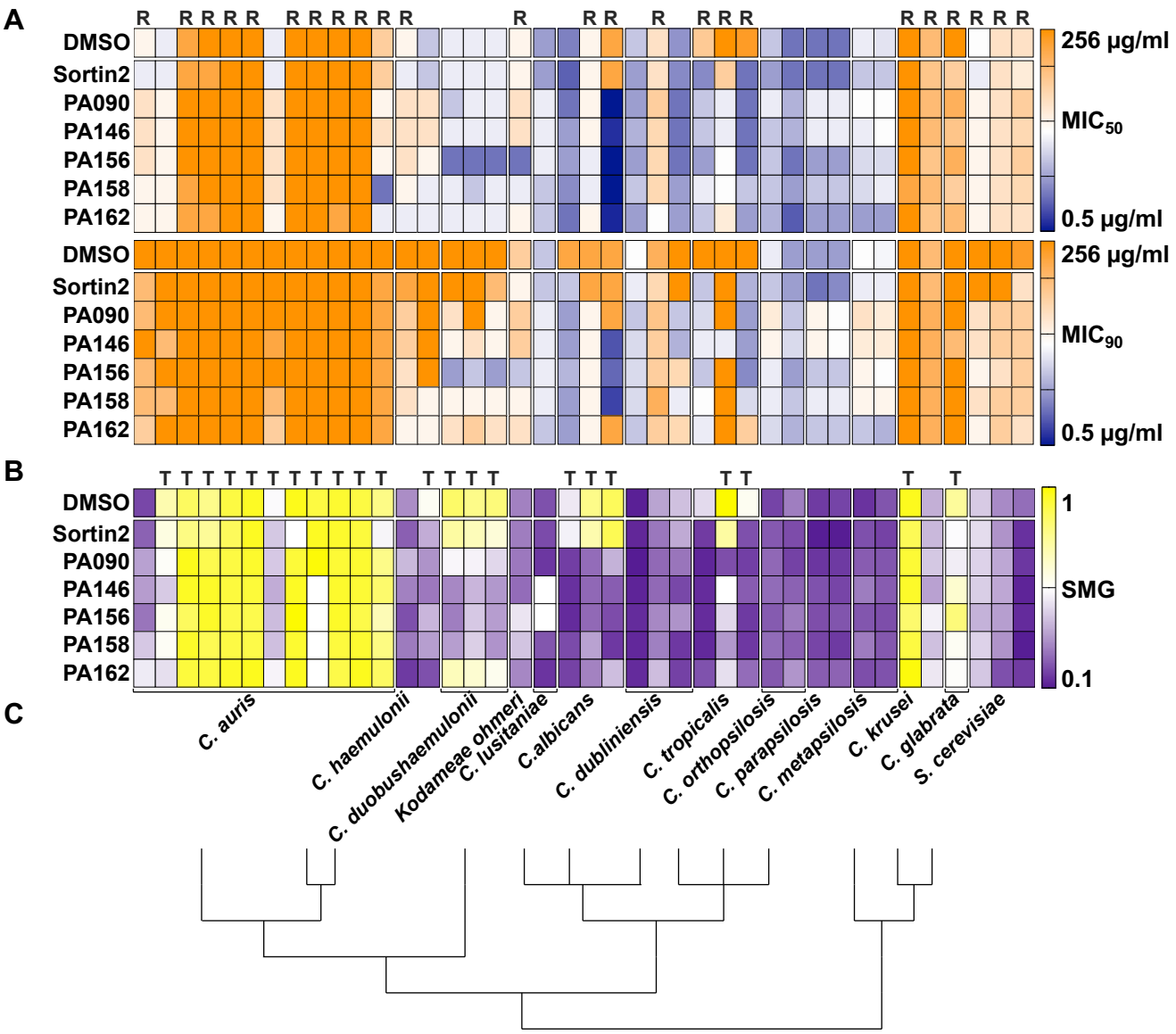
A
R R R R R R R R R R R R R R R R R R R R R R R R
DMSO
Sortin2
PA090
PA146
PA156
PA158
PA162
256 µg/ml
MIC50
0.5 µg/ml
DMSO
Sortin2
PA090
PA146
PA156
PA158
PA162
256 µg/ml
MIC90
0.5 µg/ml
B
T T T T T T T T T T T T T T T T T T T T T T T T
DMSO
Sortin2
PA090
PA146
PA156
PA158
PA162
1
SMG
0.1
C
C. auris
C. haemulonii
C. duobushaemulonii
Kodameae ohmeri
C. lusitaniae
C.albicans
C. dubliniensis
C. tropicalis
C. orthopsilosis
C. parapsilosis
C. metapsilosis
C. krusei
C. glabrata
S. cerevisiae

Figure 7.

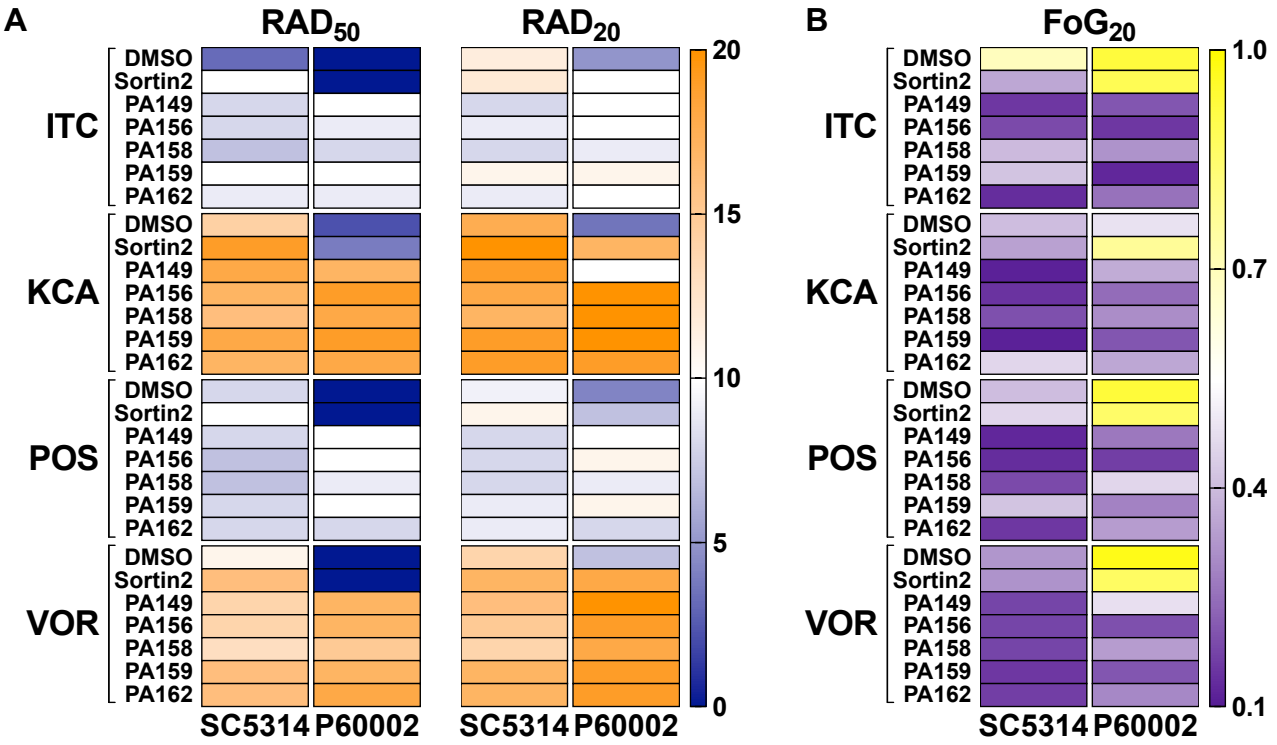
A
RAD50
RAD20
B
FoG20
ITC
KCA
POS
VOR
DMSO
Sortin2
PA149
PA156
PA158
PA159
PA162
SC5314
P60002
20
15
10
5
0
1.0
0.7
0.4
0.1

Figure 8.

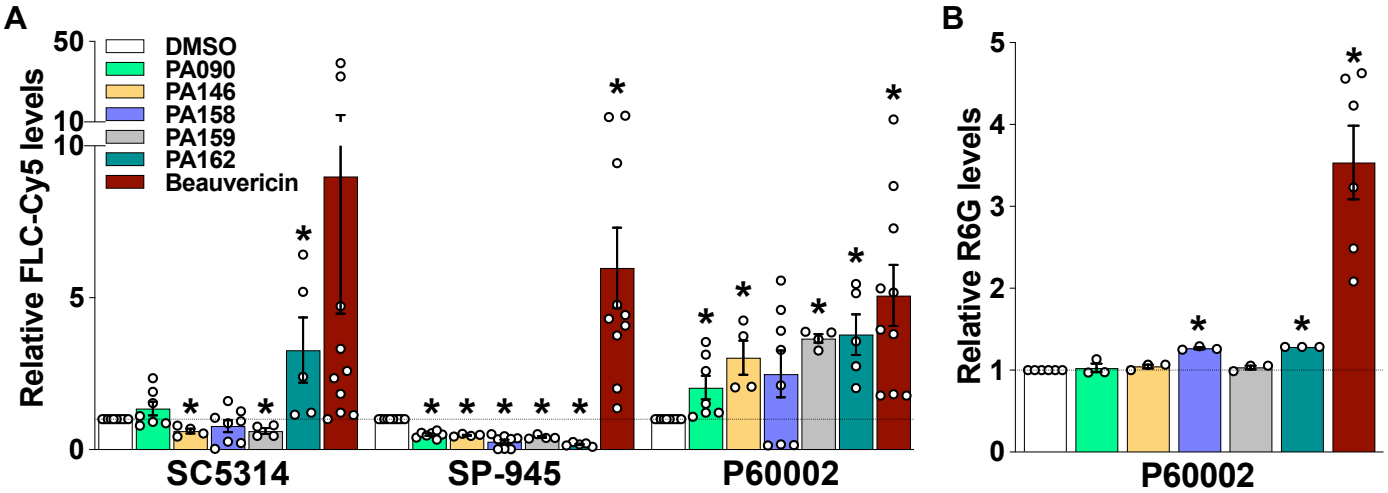
A
DMSO
PA090
PA146
PA158
PA159
PA162
Beauvericin
Relative FLC-Cy5 levels
50
10
10
5
0
SC5314
SP-945
P60002
B
Relative R6G levels
5
4
3
2
1
0
P60002

Figure 9.

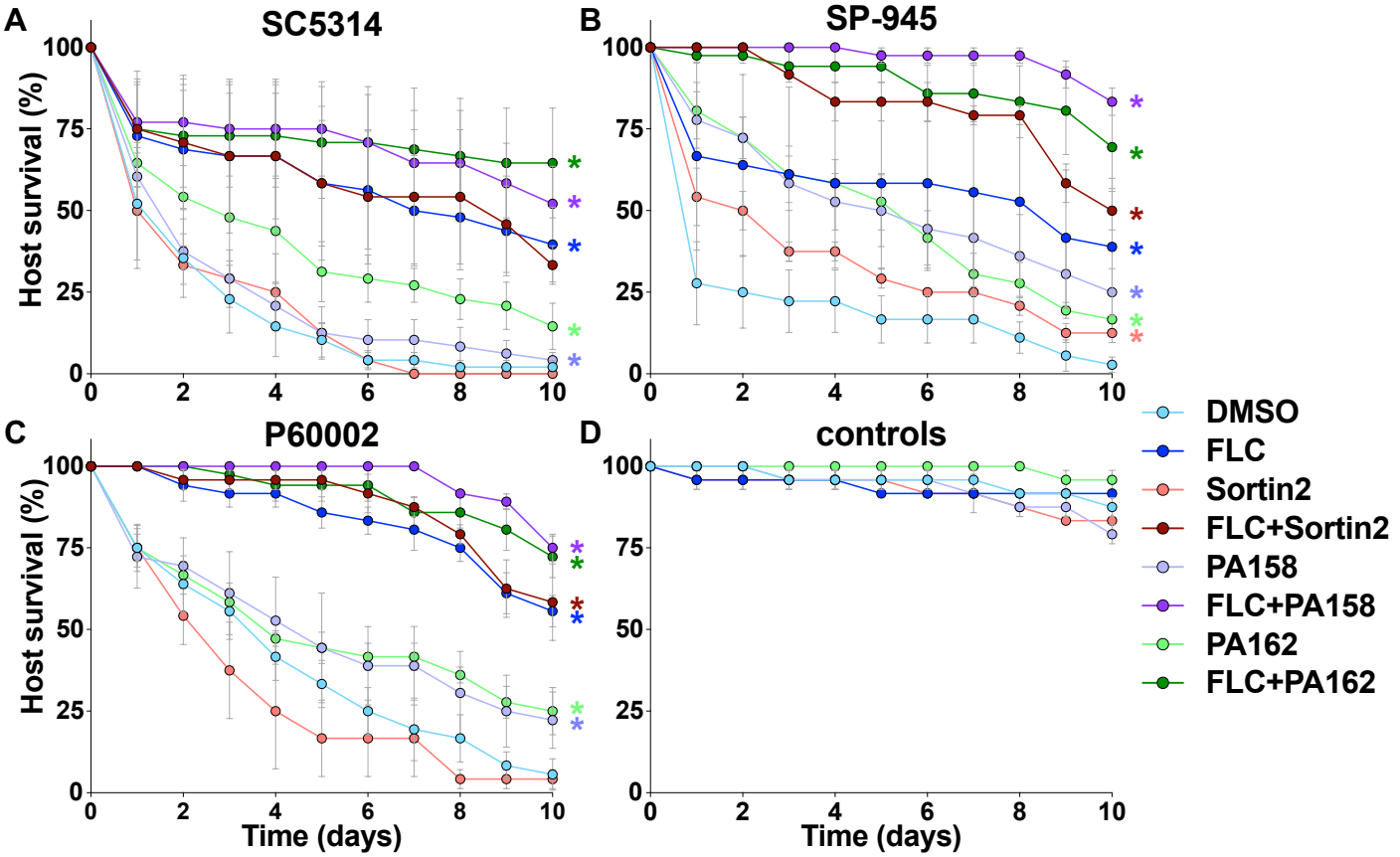
A
SC5314
B
SP-945
C
P60002
D
controls
Host survival (%)
Time (days)
DMSO
FLC
Sortin2
FLC+Sortin2
PA158
FLC+PA158
PA162
FLC+PA162